Chapter 6
Flows Instabilities

The study of the stability of flows is one of the cornerstones of Fluid Mechanics: the subject is so large that it would deserve a whole book to be reviewed. Leaving aside such an ambitious goal, we shall concentrate, in this chapter and the following one, on the fundamentals, although, here and there, making some excursions in more specialized topics.

The importance of instabilities, or stability questions, comes from their relation to turbulence and mixing. An unstable flow is a necessary path to a turbulent one. Turbulence is indeed a fundamental process in Fluid Mechanics because it controls in many circumstances the fluid transport properties. The conditions within which turbulence sets in, can be appreciated only when the questions of stability are settled. Often, this is not sufficient, but always necessary.

6.1 Local Analysis of Instabilities

When we discussed the equations of perturbations, we found that a simple way to understand their evolution was to consider them as plane waves and analyse their dispersion relation. Owing to the simplicity of the approach, we again start with this type of analysis.

6.1.1 Definitions

First of all, let us recall that the local analysis is only valid if the wavelength of disturbances is very small compared to the scales of the velocity field as given by expression (5.7).

M. Rieutord, *Fluid Dynamics*, Graduate Texts in Physics,
DOI 10.1007/978-3-319-09351-2_6

If, for some wavevectors $\mathbf{k}$ belonging to a subset of $\mathbb{R}^3$, the dispersion relation gives a frequency ω with a negative imaginary part, then there are waves whose amplitude grows exponentially with time. This is called the *absolute* or *temporal* instability. It is the most frequent case, but the opposite one also exists: if, for some real values of the frequency, the wavevector is complex, then we face a *spatial or convective instability.*

The existence of these two types of instabilities is tied to the implicit nature of the dispersion equation: $D(\omega, \mathbf{k}) = 0$. Two types of explicit solutions are thus possible:

$$\omega(\mathbf{k}) \qquad \text{or} \qquad \mathbf{k}(\omega)$$

The first are called "temporal branches" when $\mathbf{k} \in \mathbb{R}^3$, while the second ones define the "spatial branches" if $\omega \in \mathbb{R}$. For example, the dispersion relation

$$\omega + 2k - k^2 = 0$$

possesses one temporal branch $\omega = k^2 - 2k$, which is stable, and two spatial branches $k = 1 \pm \sqrt{1 + \omega}$ which can generate a spatial instability.

6.1.2 The Gravitational Instability

A simple example of an absolute instability comes from Astrophysics with the gravitational instability, which is at the origin of star formation. To make things as simple as possible, we consider an unbounded fluid of uniform temperature and pressure. We assume that it is an ideal gas of adiabatic index γ. The sound waves propagate with a velocity

$$c_s = \sqrt{\gamma P_0 / \rho_0}$$

where P_0 and ρ_0 are respectively the pressure and density of the undisturbed medium.

The linearized equations satisfied by the disturbances of the medium are:

$$\begin{cases} \dfrac{\partial \delta\rho}{\partial t} + \rho_0 \nabla \cdot \mathbf{v} = 0 \\[2ex] \rho_0 \dfrac{\partial \mathbf{v}}{\partial t} = -\nabla \delta P - \rho_0 \nabla \delta \Phi \\[2ex] \delta P = c_s^2 \delta\rho \\[2ex] \Delta \delta \Phi = 4\pi G \delta\rho \end{cases} \tag{6.1}$$

where we have taken into account the fluctuations in the gravitational field generated by the fluctuations of density (the last equation of the system). For plane wave solutions

$$\delta\rho = \delta\rho_0 e^{i(\omega t+\mathbf{k}\cdot\mathbf{r})}, \quad \mathbf{v} = \mathbf{v}_0 e^{i(\omega t+\mathbf{k}\cdot\mathbf{r})}, \text{ etc.} \tag{6.2}$$

we find the following dispersion relation:

$$\omega^2 = c_s^2 k^2 - 4\pi G\rho_0 \tag{6.3}$$

This relation clearly shows a temporal instability since all the perturbations with a wavenumber smaller than

$$k_J = \sqrt{\frac{4\pi G\rho_0}{c_s^2}} \tag{6.4}$$

are unstable and grow exponentially. The associated wavelength $\lambda_J = 2\pi/k_J$ is called *Jeans' length* and the associated criterion, *Jeans' criterion*. The dispersion relation (6.3) also shows that there is no spatial instability:

$$c_s^2 k^2 = \omega^2 + 4\pi G\rho_0 > 0, \quad \forall\omega \in \mathbb{R};$$

thus k is always real.

In order to fix ideas, let us calculate Jeans' length in the case of the Earth's atmosphere. We assume it to be a mass of air at $P_0 = 10^5$ Pa and $T_0 = 20\,°\text{C}$. Then, $c_s = 343$ m/s and ρ_0= 1.2 kg/m^3 giving $\lambda_J = 6.8\,10^4$ km. The Earth's atmosphere, much smaller (in thickness) than this length, is not, therefore, in danger of gravitational collapse! On the other hand, an interstellar cloud of a hundred solar masses,[1] with a temperature of 50 K and a diameter of two light-years can be wiped out gravitationally (see exercises).

The example of the Earth's atmosphere is interesting as it points out the limits of the local analysis: if the dimensions of the fluid domain are smaller than the wavelength of the disturbances we are interested in, the local solutions are invalid because of boundary conditions.

6.1.3 Convective Instability

Such an instability is usually found in shear flows, for instance in a boundary layer. Perturbations are amplified in the downstream direction and may transform a laminar flow into a turbulent one (see Fig. 6.14 for the growth of a perturbation in

[1] A solar mass, symbolized by $M_\odot$, is equal to 2×10^{30} kg.

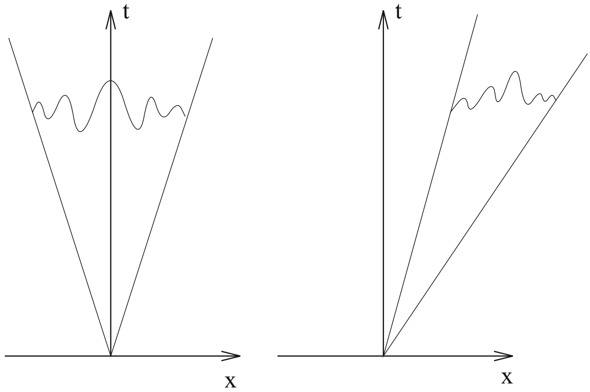

Fig. 6.1 Sketch of an absolute (*left*) and convective (*right*) instability in the (x, t)-plane

the downstream direction). This instability can also be regarded as the growth of an absolute instability advected by the background flow as shown in Fig. 6.1.

To further illustrate this mechanism, we shall consider a model problem based on the perturbations of Burgers flow.[2] The background flow is uniform and disturbances are only on the velocity field and one-dimensional; thus $\delta\mathbf{u} = \delta u(x, t)\mathbf{e}_x$ and

$$\frac{\partial \delta u}{\partial t} + U\frac{\partial \delta u}{\partial x} = \nu\frac{\partial^2 \delta u}{\partial x^2}$$

where ν is the kinematic viscosity. The dispersion relation of the Fourier modes is

$$i\omega + ikU = -\nu k^2$$

This relation immediately shows that the temporal branch is stable since, for a given k, the temporal dependence $\exp(i\omega t)$ leads to an exponential decay.

Let us now extract the spatial branches of this dispersion relation. We easily find that two branches exist, namely

$$k_\pm = \frac{iU}{2\nu}\left(1 \pm \sqrt{1 + \frac{4i\omega\nu}{U^2}}\right)$$

To discuss its properties, it is convenient to consider the limiting case of a small viscosity such that $\omega\nu \ll U^2$. Thus,

$$k_+ = -\frac{\omega}{U} + \frac{iU}{\nu} \qquad \text{and} \qquad k_- = \frac{\omega}{U} - \frac{2i\nu\omega^2}{U^3}$$

[2]Burgers equation is given by (5.85).

To see whether these branches correspond to growing or decaying perturbations, it is useful to write the resulting velocity field, namely

$$\mathbf{u}^+ = \mathbf{u}_0^+ e^{\frac{i\omega}{U}(x+Ut)+\frac{U}{\nu}x} \qquad \text{and} \qquad \mathbf{u}^- = \mathbf{u}_0^- e^{-\frac{i\omega}{U}(x-Ut)-\frac{2\nu\omega^2}{U^3}x}$$

These expressions show that a given phase of $\mathbf{u}^+$ propagate to negative values of x, therefore its amplitude decreases rapidly as $\exp(Ux/\nu)$. On the other hand the phase of $\mathbf{u}^-$ propagates to positive values of x, and its amplitude also decreases (but slower, as $\exp(-\nu\omega^2 x/U^3)$) as the perturbation moves to high values of x. In this example, we see that if some disturbance is forced at a given frequency ω at $x = 0$ say, it will propagate upstream and downstream, but both waves will be damped. Thus the flow is stable.

6.2 Linear Analysis of Global Instabilities

Although local analysis is very handy to get a first impression of the stability of a steady flow, it is often limited in its applications because of the boundary conditions. To deal with this constraint, we need moving to the global analysis, which is often difficult. A medium way is to take into account the boundary conditions only in one direction. Although still quite idealized, the resulting solutions are usually very instructive on the physics of the flow. With this approach, we shall investigate selected examples of instabilities, which will enlight us, at the same time, on the properties of rotating fluids, shear flows, etc.

6.2.1 Centrifugal Instability: Rayleigh's Criterion

Let us consider a perfect incompressible fluid filling the gap between two cylinders of radii R_1 and R_2. The fluid rotates with the prescribed angular velocity profile $\Omega(s)$. We wish to know the conditions to be met by this rotation law, for this flow to be stable or unstable. The original flow, $\mathbf{U} = s\Omega(s)\mathbf{e}_\varphi$, is a solution of Euler's equation and satisfies $\nabla \cdot \mathbf{U} = 0$.

To simplify the analysis, we assume that the cylinders are infinitely long. Thus, boundary conditions are only imposed in the radial direction and we are allowed to make a local analysis in the z-direction. We further restrict the disturbances to the axisymmetric ones; we thus write the perturbations of the velocity and pressure fields as

$$\mathbf{u}(s,z,t) = \mathbf{u}(s)e^{ikz+\lambda t}, \qquad P(s,z,t) = \rho p(s)e^{ikz+\lambda t} \tag{6.5}$$

where ρ is the fluid density.

6.2.1.1 Equations for the Perturbations

The momentum equation leads to the following equations for $p(s)$ and $\mathbf{u}(s)$:

$$\lambda \mathbf{u} + (\mathbf{U} \cdot \nabla)\mathbf{u} + (\mathbf{u} \cdot \nabla)\mathbf{U} = -\nabla p \tag{6.6}$$

which we rewrite as

$$\lambda \mathbf{u} - 2\Omega(s) u_\varphi \mathbf{e}_s + (\Omega(s) u_s + (\mathbf{u} \cdot \nabla) U(s)) \mathbf{e}_\varphi = -\nabla p \; . \tag{6.7}$$

with cylindrical coordinates (s, φ, z).

Finally, taking mass conservation into account, we get the four following equations:

$$\begin{cases} \lambda u_s - 2\Omega(s) u_\varphi = -\dfrac{dp}{ds} \\ \lambda u_\varphi + \Phi_1(s) u_s = 0 \\ \lambda u_z = -ikp \\ \dfrac{1}{s}\dfrac{d}{ds}(s u_s) + iku_z = 0 \end{cases} \tag{6.8}$$

where we have introduced

$$\Phi_1(s) = \frac{1}{s}\frac{d(s^2\Omega)}{ds} \; .$$

The second equation gives the expression of u_φ as a function of u_s. The third and fourth ones relate p and u_s. Altogether they lead to a single equation for u_s now denoted u, namely

$$\frac{d}{ds}\left[\frac{1}{s}\frac{d(su)}{ds}\right] - k^2 u = \frac{k^2}{\lambda^2}\kappa^2(s) u \tag{6.9}$$

where

$$\kappa^2(s) = 2\Omega \Phi_1 = \frac{1}{s^3}\frac{d(s^2\Omega)^2}{ds} \tag{6.10}$$

is proportional to the radial derivative of the angular momentum $\ell = s^2\Omega$ of the fluid particles in the original flow. $\kappa(s)$ is called the *epicyclic frequency*. We shall comment later about its physical meaning.

Setting, $\Lambda = 1/\lambda^2$, the differential equation (6.9) has the general and interesting form:

$$\mathcal{L}u = \Lambda k^2 \Phi(s) u \tag{6.11}$$

Supplemented with the boundary conditions $u = 0$ at $s = R_1$ and $s = R_2$, this is the classical Sturm–Liouville problem in the theory of differential equations. We refer the reader to the maths complements in Chap. 12 to get acquainted with the basic properties of Sturm–Liouville problems and proceed to the consequences for our problem.

6.2.1.2 The Rayleigh Criterion

First of all, let us compare (6.11) with the general equation (5.11): it is of the same form. Thus, in order to determine the stability of the flow **U**, we "just" need to know the spectrum of the operator $k^{-2}\Phi(s)^{-1}\mathcal{L}$, which gives the set of allowed values of Λ. Usually, this is not an easy game; however, because of the Sturm–Liouville nature of the eigenvalue problem, the answer is straightforward. For such problems indeed, it may be shown that the eigenvalues are discrete, real and of the sign of $-k^2\Phi(s)$ if this function keeps the same sign in the interval of definition $[R_1, R_2]$. If Φ changes sign the eigenvalues are of both signs.

These properties of the Sturm–Liouville problems allow us to conclude on the stability of the flow. Indeed, if $\Phi(s) \geq 0$, all the eigenvalues Λ are negative, which means that all the eigenvalues λ are purely imaginary. Thus perturbations are just neutral; the flow is stable. On the other hand, if there exist an interval where Φ is negative, then there exist some eigenvalues Λ that are positive, implying the existence of real positive λ, and thus the existence of amplified disturbances making the flow unstable.

The foregoing result shows that the flow under consideration is unstable when, somewhere, the specific angular momentum ℓ decreases with r (making $\Phi < 0$). In this case, some axisymmetric disturbances grow exponentially. The opposite situation, where $\Phi(s) \geq 0$, does not mean that the flow is stable; it means that axisymmetric disturbances are not amplified, however, some non-axisymmetric ones could be growing.

We thus find *a sufficient condition* for an instability ($\Phi(s) < 0$ somewhere) or *a necessary condition* for stability ($\Phi(s) \geq 0$ everywhere). This criterion was discovered by Rayleigh and named after him.

6.2.1.3 The Rayleigh Criterion: A Heuristic Derivation

The foregoing argument is rather mathematical and little intuitive. However, the result may be explained on more physical grounds as follows. Let us consider two annular fluid elements of radii s_1 and s_2, with $s_1 < s_2$. Their angular momentum is respectively ℓ_1 and ℓ_2. Their total kinetic energy is

$$E_k = \frac{1}{2}\left(\frac{\ell_1^2}{s_1^2} + \frac{\ell_2^2}{s_2^2}\right)$$

Now let's suppose that the position of these two fluid elements is inverted: their angular momentum and mass are conserved, but the kinetic energy of the two elements is now

$$E_k' = \frac{1}{2}\left(\frac{\ell_1^2}{s_2^2} + \frac{\ell_2^2}{s_1^2}\right)$$

Making the difference between these two expressions, we find

$$E_k - E_k' = \frac{1}{2}\left(\ell_2^2 - \ell_1^2\right)\left(\frac{1}{s_2^2} - \frac{1}{s_1^2}\right)$$

If the angular momentum increases outwards then $\ell_2 > \ell_1$ and $E_k < E_k'$, therefore the change imposed is energetically unfavorable: the situation is stable. If, in the opposite case, the angular momentum decreases outwards then $\ell_2 < \ell_1$ and $E_k > E_k'$: some energy is released if the position of the fluid elements are interchanged. The system cannot stay in its initial configuration and will evolve towards a new state of lower energy.

6.2.2 Shear Instabilities of Parallel Flows

Parallel shear flows represent a vast category of flows that are very common in Nature and often at the origin of turbulence. A parallel shear flow is basically very simple: its velocity field is like:

$$\mathbf{V} = U(z)\mathbf{e}_x\,. \tag{6.12}$$

It has only one component, taken here in the x-direction, which is a function of only one coordinate normal to the direction of the flow, here z. We only consider steady flows. We note that, if the density of the fluid is independent of the coordinate in the velocity direction then, the equation of continuity is automatically satisfied. To further simplify, we restrict our discussion to the case of incompressible fluids.

The stability of parallel shear flows has an interesting property formulated by *Squire's theorem*: the most unstable disturbances of these flows are two-dimensional. This greatly simplifies the analysis of the stability of such flows. We shall therefore start by proving this theorem before presenting some famous examples of shear instabilities.

6.2.2.1 Squire's Theorem

Statement: *To every unstable disturbance of a parallel shear flow of an incompressible fluid there corresponds a more unstable two-dimensional disturbance.*
Proof: We begin by proving this theorem in the inviscid case. We assume that the perturbations are in the following form:

$$f(\mathbf{r},t) = f(z)e^{ik_x x + ik_y y + \lambda t} \tag{6.13}$$

where the Fourier form is in the homogenous directions of the flow. The perturbations satisfy

$$\begin{cases} \dfrac{\partial \mathbf{v}}{\partial t} + U(z)\dfrac{\partial \mathbf{v}}{\partial x} + v_z U'(z)\mathbf{e}_x = -\boldsymbol{\nabla} P \\ \\ \boldsymbol{\nabla} \cdot \mathbf{v} = 0 \end{cases} \tag{6.14}$$

After substitution by (6.13) and projection along the three axes, we find

$$\begin{cases} (\lambda + ik_x U)v_x + v_z U'(z) = -ik_x P \\ (\lambda + ik_x U)v_y = -ik_y P \\ (\lambda + ik_x U)v_z = -DP \\ Dv_z + ik_x v_x + ik_y v_y = 0 \end{cases} \tag{6.15}$$

where we have set $D = \frac{\partial}{\partial z}$. We now make *Squire's transformation* and set

$$\tilde{k} = \sqrt{k_x^2 + k_y^2}, \qquad \tilde{k}\tilde{v} = k_x v_x + k_y v_y, \qquad \tilde{P} = \frac{\tilde{k}}{k_x} P$$

The equations are now

$$\begin{cases} (\lambda + ik_x U)\tilde{v} + \dfrac{k_x}{\tilde{k}} v_z U'(z) = -i\tilde{k} P \\ \\ (\lambda + ik_x U)v_z = -\dfrac{k_x}{\tilde{k}} D\tilde{P} \\ \\ Dv_z + i\tilde{k}\tilde{v} = 0 \end{cases} \tag{6.16}$$

which can again be written as

$$\begin{cases} (\tilde{\lambda} + i\tilde{k}U)\tilde{v} + v_z U'(z) = -i\tilde{k}\tilde{P} \\ (\tilde{\lambda} + i\tilde{k}U)v_z = -D\tilde{P} \\ Dv_z + i\tilde{k}\tilde{v} = 0 \end{cases} \tag{6.17}$$

by introducing $\tilde{\lambda} = \lambda \frac{\tilde{k}}{k_x}$. Noting the similarity of (6.17) and (6.15) with $k_y = v_y = 0$, we conclude that, if the flow is unstable, namely if $Re(\lambda) > 0$, for every three-dimensional disturbance, we can construct a two-dimensional disturbance $(\tilde{v}, v_z, \tilde{P})$ that grows faster, since $Re(\tilde{\lambda}) \geq Re(\lambda)$.

The case with viscosity is treated in a similar manner. While observing that for the disturbances (6.13), the Laplacian is changed into $D^2 - \tilde{k}^2$, we rewrite (6.15) in the form

$$\begin{cases} [\lambda + ik_x U - \nu(D^2 - \tilde{k}^2)]v_x + v_z U'(z) = -ik_x P \\ [\lambda + ik_x U - \nu(D^2 - \tilde{k}^2)]v_y = -ik_y P \\ [\lambda + ik_x U - \nu(D^2 - \tilde{k}^2)]v_z = -DP \\ Dv_z + ik_x v_x + ik_y v_y = 0 \end{cases} \tag{6.18}$$

We apply Squire's transformation

$$\begin{cases} [\tilde{\lambda} + i\tilde{k}U - \tilde{\nu}(D^2 - \tilde{k}^2)]\tilde{v} + v_z U'(z) = -i\tilde{k}\tilde{P} \\ [\tilde{\lambda} + i\tilde{k}U - \tilde{\nu}(D^2 - \tilde{k}^2)]v_z = -D\tilde{P} \\ Dv_z + i\tilde{k}\tilde{v} = 0 \end{cases} \tag{6.19}$$

where $\tilde{\nu} = \nu \frac{\tilde{k}}{k_x} \geq \nu$. Thus, with every three-dimensional disturbances, we can associate a two-dimensional disturbance, for which the Reynolds number is smaller. Consequently, the critical Reynolds number, above which a given perturbation grows exponentially, can be decreased by applying Squire's transformation to that perturbation. Hence, the perturbations, which give the lowest critical Reynolds number of shear flows, are the two-dimensional ones.

6.2.3 Rayleigh's Equation

In order to complete our study of parallel shear flows, we now transform (6.15) into an ordinary differential equation for the stream function of the disturbances, since, thanks to Squire's theorem, we can restrict our study to two-dimensional perturbations only. Accordingly, we set

$$v_x = \frac{\partial \psi}{\partial z} = D\psi \qquad \text{and} \qquad v_z = -\frac{\partial \psi}{\partial x} = -ik\psi$$

where $k = k_x$ and $k_y = 0$. We then transform (6.15) into

$$(\lambda + ikU)k^2\psi = D\left[(\lambda + ikU)D\psi - ik\psi U'\right]$$

then finally into

$$(\lambda + ikU)(D^2 - k^2)\psi - ikU''\psi = 0 \tag{6.20}$$

which is Rayleigh's equation.

6.2.3.1 Criteria of Stability

We can infer from Rayleigh's equation a necessary condition for instability, that is to say, a condition so that $Re(\lambda) > 0$ is possible. We return to (6.20) and assume that the fluid is bounded by two planes located in $z = a$ and $z = b$. By integrating the equation over this domain after multiplication it by ψ^*, the complex conjugate of ψ, we find

$$\int_a^b \psi^*(D^2 - k^2)\psi dz - ik \int_a^b \frac{U''|\psi|^2}{\lambda + ikU} dz = 0 \; .$$

Since $v_z = 0$ on each bounding plane, integration by parts yields

$$\int_a^b (|D\psi|^2 + k^2|\psi|^2) dz + ik \int_a^b \frac{U''|\psi|^2}{\lambda + ikU} dz = 0 \tag{6.21}$$

The imaginary part of this equation leads to

$$Re(\lambda)k \int_a^b \frac{|\psi|^2 U''}{|\lambda + ikU|^2} dz = 0 \tag{6.22}$$

which shows that a necessary condition for the existence of an instability is that the integral be zero. This condition implies that U'' changes sign at least once in the interval $[a, b]$. Reciprocally, this condition shows that if a velocity profile has no point of inflexion, then $Re(\lambda) = 0$ and the flow is stable with respect to infinitesimal disturbances.

This condition is evidently not sufficient: even if $Re(\lambda) \neq 0$, this quantity is not necessarily positive!

Rayleigh proved this result in 1880. In 1950 Fjørtoft found a more constraining version of it. He showed that a necessary condition for instability was that

$$U''(U - U_i) < 0$$

at some point in the flow where U_i is the velocity at the inflexion point. We propose the proof of this theorem as part of the exercises.

6.2.4 The Orr–Sommerfeld Equation

The Orr–Sommerfeld equation is the variant of Rayleigh's equation including viscosity. We obtain this equation after several manipulations of (6.19), by expressing v_x and v_z with the help of the stream function. Orr–Sommerfeld equation has the following form:

$$\left(\lambda + ikU - \nu(D^2 - k^2)\right)(D^2 - k^2)\psi = ikU''\psi \tag{6.23}$$

which we complete with the no-slip boundary conditions at the walls (planes $z = 0$ and $z = d$), namely

$$\psi = D\psi = 0 \qquad \text{at} \qquad z = 0 \qquad \text{and} \qquad z = d$$

We shall not discuss the solutions of this equation because it would bring us too far, and refer the interested reader to the book of Drazin and Reid (1981). We shall give a few comments only.

Shear flows, like boundary layers, jets, wakes, mixing layers, etc. are usually the seat of strong turbulence, which is a consequence of shear instabilities. The Orr–Sommerfeld equation offers a nice model to study these instabilities and its solutions have therefore numerous applications.

Many cases have been studied. The simplest ones are those at low Reynolds number, which can be investigated by perturbation methods on the diffusion equation. However, they are not the most interesting since applications usually require the other extreme: a very high Reynolds number. As we saw in Chap. 4, this implies the existence of boundary layers, but not only. Indeed, from Rayleigh equation, to which Orr–Sommerfeld reduces at infinite Reynolds number, we observe that something special must occur when

$$\lambda + ikU = 0$$

or when $c = \frac{\omega}{k} = -U$. This equality means that the phase velocity of the perturbations is equal and opposite to the fluid velocity; the phase perturbation stands still in the reference frame. At this place, the coefficient of the second derivatives of ψ vanishes. A singularity of the perturbed flow shows up: this is *a critical layer*. In such a layer, viscosity smooths out the singularity, which usually consists in a discontinuity of the parallel component of the velocity field (see Sect. 6.3.3 for instance). Critical layer are also called *detached shear layers*; their thickness, like the one of boundary layers, scales like some fractional power of the viscosity ($\nu^{1/3}$ and $\nu^{1/4}$ are the most common cases). They are important in the global dynamics of a fluid layer as they are strong dissipative structures.

Ending the chapter, we shall use Orr–Sommerfeld equation to introduce algebraic instabilities that represent another path to turbulent flows.

6.3 Some Examples of Famous Instabilities

6.3.1 *Example: The Kelvin–Helmholtz Instability*

The Kelvin–Helmholtz instability is a shear instability that appears when two fluid layers of different densities, slide one on the other.

In order to analyse this instability, we shall consider the setup of an air flow on top of a water plane. *The two fluids are assumed to be inviscid.* The air occupies the $z > 0$ half-space, while the water fills the remaining space. The air is assumed to be moving at a constant velocity $V\mathbf{e}_x$ with respect to the water. To be complete, we also take into account the surface tension γ between the two fluids. Thus, except for the air motion, the set-up is exactly the same as the one use in Sect. 5.3, when studying surface waves.

As in Sect. 5.3, we assume the perturbations of the velocity field to be irrotational, namely $\delta\mathbf{v} = \nabla\Phi_a$. We thus rewrite the second equation of (5.26) directly as:

$$\frac{\partial \Phi_a}{\partial t} + V\frac{\partial \Phi_a}{\partial x} + \frac{\delta P_a}{\rho_a} + g\delta z = cst \tag{6.24}$$

Since the potential Φ_a still satisfies Laplace's equation, (5.29) is always satisfied because we are still looking for solutions in the form of (5.27). On the other hand the boundary condition (5.30) is modified on the air side, indeed

$$v_{z,water} = \frac{\partial z_s}{\partial t} \qquad \text{and} \qquad v_{z,air} = \frac{\partial z_s}{\partial t} + V\frac{\partial z_s}{\partial x}$$

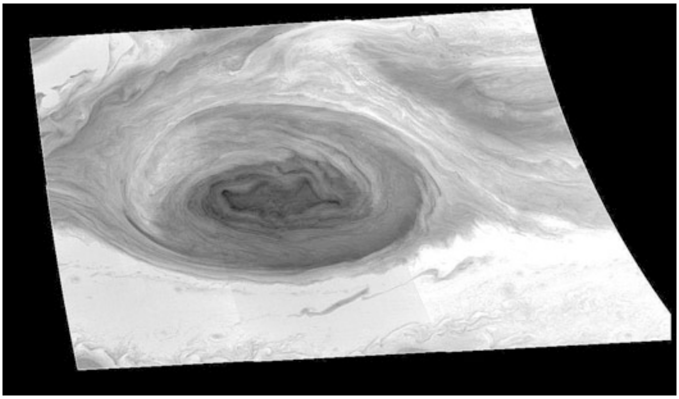

Fig. 6.2 The great red spot of Jupiter as viewed by the Galileo probe. Note the vortices around it. They come from the shear instabilities forced by this flow (Credit NASA)

(5.32) is therefore replaced by

$$k\Phi_{water}(0) = -i\omega z_s \qquad \text{and} \qquad k\Phi_a(0) = i(\omega - kV)z_s$$

Since we take surface tension into account we have

$$\delta P_w = \delta P_a + \gamma k^2 z_s$$

according to (5.40). Finally, we derive the following dispersion relation

$$\omega^2(\rho_w + \rho_a) - 2\omega\rho_a kV - (\rho_w - \rho_a)gk - \gamma k^3 + \rho_a k^2 V^2 = 0 \tag{6.25}$$

The temporal branches can be easily extracted:

$$\omega_\pm = \frac{kV\rho_a \pm \sqrt{\Delta}}{\rho_w + \rho_a} \qquad \text{and} \qquad \Delta = (\rho_w + \rho_a)[k^3\gamma + (\rho_w - \rho_a)gk] - k^2V^2\rho_a\rho_w \tag{6.26}$$

The expression of $\omega_\pm$ shows that the instability arises when $\Delta < 0$, that is when

$$V^2 > \frac{\rho_w + \rho_a}{\rho_a\rho_w}\left[\gamma k + (\rho_w - \rho_a)\frac{g}{k}\right] .$$

Since the term in brackets has a minimum when $k = k_{min} = \sqrt{(\rho_w - \rho_a)g/\gamma}$, we see that the flow will be unstable if, and only if, the velocity V is greater than the critical velocity given by:

$$V_{crit} = \left(\frac{2}{\rho_w} + \frac{2}{\rho_a}\right)^{1/2} [\gamma g(\rho_w - \rho_a)]^{1/4} \tag{6.27}$$

With typical values of a water-air interface, namely $\rho_w = 1{,}000\,\text{kg/m}^3$, $\rho_a = 1.2\,\text{kg/m}^3$, $g = 9.81\,\text{m/s}^2$ and $\gamma = 0.072\,\text{N/m}$, we find $V_{crit} = 6.4\,\text{m/s}$. The wavelength of the most unstable mode, namely that for which $k = k_{min}$, is $\lambda_{crit} = 1.7$ cm, which is the length where the capillary effects are of the same order of magnitude as those of gravity (see Sect. 5.3.2).

6.3.2 Instabilities Related to Kelvin–Helmholtz Instability

Formula (6.25) actually contains many interesting cases that we shall discuss now.

6.3.2.1 Rayleigh–Taylor Instability

If in (6.25) we set $V = 0$, we immediately find the dispersion relation of gravity or capillary waves (5.43). Now, let us assume that we manage to put the water above the air. This situation is likely unstable. In fact, since

$$\omega^2 = \frac{(\rho_a - \rho_w)gk + \gamma k^3}{\rho_e + \rho_a} , \tag{6.28}$$

we see that this is not necessarily the case. In order for the situation to be unstable, it is necessary that $k < \sqrt{(\rho_w - \rho_a)g/\gamma}$, namely that the perturbations with a wavelength greater than $\lambda_{crit} = 2\pi\sqrt{\gamma/(\rho_w - \rho_a)g}$ can grow.

The foregoing instability, which appears when a layer of fluid covers a layer of a less dense fluid in a gravitational field, is known as Rayleigh–Taylor instability. It usually occurs in Nature when a fluid layer is heated from the bottom. The instability then leads to a fluid flow known as thermal convection, which we shall study in detail in Chap. 7.

Now, the instability shown by (6.28) can be illustrated by a simple experiment. Taking a bottle filled with water, we turn it upside down, maintaining the cork on the orifice. Removing it delicately, we observe that if the diameter of the bottleneck is small enough,[3] the water remains in the bottle. If the diameter is too large, however, the stability of the equilibrium can be restored by increasing artificially the surface tension: a piece of paper laid on the interface will do the job.

Finally, let us note that if the surface tension is zero, for example if both fluids are gases, then the equilibrium is always unstable.

Figure 6.3 shows the development of Rayleigh–Taylor instability in a numerical simulation of a supernova explosion. This instability plays an important role in the mixing of elements yielded by this stellar explosion.

6.3.2.2 The Instability of the Mixing Layer

Another example that is easily derived from (6.25) is the one where the two fluids are identical. Thus, $\rho_a = \rho_w = \rho$.

The configuration thus obtained is the famous "vortex sheet" presented in Fig. 3.9 where the velocity sustains a discontinuity that usually develops into vortices (see Fig. 6.2). From (6.25) we see that such a configuration is unstable for all wavelengths since

$$\omega = (1 \pm i)kV/2 .$$

[3] We may expect that if the diameter of the bottleneck is smaller than 1.7 cm, the equilibrium is stable. However, we should keep in mind that the value was derived for pure water; impurities decrease the surface tension and lead to a smaller value of the critical wavelength.

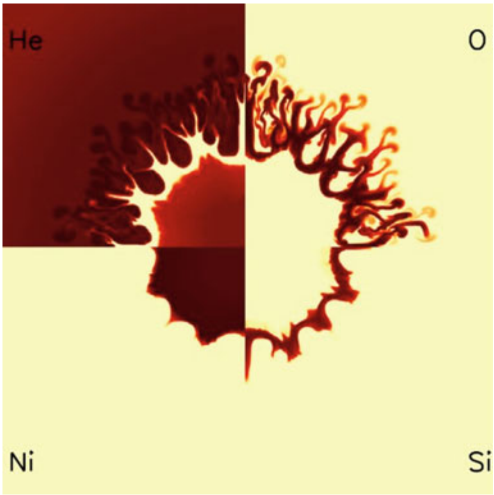

Fig. 6.3 Growth of the Rayleigh–Taylor instability in the wake of the shock wave associated with a supernova explosion. The four quadrants show the concentration of helium, oxygen, nickel and silicium. The numerical simulation has been made by Joggerst et al. (2010)

The growth rate increases with the wavenumber without bounds apparently. This dispersion relation comes from the discontinuity of the velocity field. In real systems, the discontinuity has some thickness (due to viscosity) and the growth rate reaches a maximum for perturbations with a wavelength similar to the thickness of the vortex sheet.

6.3.3 Disturbances of the Plane Couette Flow

The plane Couette flow is a shear flow for which the profile is linear:

$$U(z) = z/T \tag{6.29}$$

where T is a constant homogenous to a time. A discussion of the perturbations of this flow is interesting. Setting $\lambda = i\omega$ with $\omega \in \mathbb{R}$ and substituting (6.29) in Rayleigh's equation we find

$$(\omega + kU)(D^2 - k^2)\psi = 0 \tag{6.30}$$

If we assume that $(\omega + kU) \neq 0$, then ψ is given by

$$\psi = A\,\mathrm{sh}\,(kz + Q)$$

If the flow takes place between two planes situated at $z = 0$ and $z = d$, at which the disturbances vanish, then $\psi = 0$ throughout. Therefore, in order that the perturbations exist, it is necessary that $\omega + kz/T = 0$ in the interval $[0, d]$. In other words, the disturbances are such that

$$\omega \in [-kd/T, 0]$$

so that their spectrum is continuous.

The form of the solutions is always given by (6.30), but the solutions have a discontinuity in $z = z_c = -\omega T/k$. Actually, we have

$$\psi(z) = A \operatorname{sh} kz, \qquad \text{if} \quad 0 \le z \le z_c$$

$$\psi(z) = B \operatorname{sh} k(z-d), \qquad \text{if} \quad z_c \le z \le d$$

At $z = z_c$, ψ is continuous because v_z is continuous, which is imposed by mass conservation. Therefore, we have

$$B = A \frac{\operatorname{sh} kz_c}{\operatorname{sh} k(z_c - d)}$$

Let us now calculate $v_x = D\psi$ on each side of z_c. We easily verify that $v_x(z_c^-) \neq v_x(z_c^+)$. The component v_x is discontinuous at this point. This discontinuity illustrates a property of linear operators, which connects the existence of a continuous spectrum to that of discontinuous eigenfunctions.

This discontinuity of the perturbed v_x means that the plane Couette flow is likely unstable to finite-amplitude disturbances. Indeed, such a perturbation will contain a vortex sheet, which is always unstable. This inference has been actually verified experimentally and numerically.

6.3.4 Shear and Stratification

To conclude this section on famous unstable shear flows, we now study the case where the fluid is stably stratified in the vertical direction. In this way, we can examine the case where shear instabilities are opposed by a positive temperature gradient that inhibits vertical motions but allows the propagation of internal gravity waves. This situation is often met in natural systems, for instance a lake over which a wind is blowing. The wind entrains surface water and thus imposes some shear flow in the lake. But lake water is often stably stratified with cold (dense) water below (light) warmer water. Because of this stratification, shear flow instabilities may be inhibited, and thus the mixing of waters in the lake.

In order to study the evolution of disturbances in such a system, we return to (6.14) modified to take the buoyancy force into account and completed by the equation of temperature (5.45b).

Staying with the two-dimensional case and using the same notations as before, we now have:

$$\begin{cases} (\lambda + ikU)v_x + U'v_z = -ikP \\ (\lambda + ikU)v_z = -DP + \alpha g T \\ (\lambda + ikU)T + v_z \partial_z T_0 = 0 \\ Dv_z + ikv_x = 0 \end{cases} \tag{6.31}$$

where T is the temperature fluctuation, α the coefficient of thermal expansion (see 1.60) and T_0 is the background temperature profile of the fluid in equilibrium. We also introduce the Brunt–Väisälä frequency N such that $N^2 = \alpha g \partial_z T_0$ and the stream function ψ such that $v_x = D\psi$ and $v_z = -ik\psi$. We can then cast the preceding system into a single equation for ψ:

$$(\lambda + ikU)[D^2 - k^2]\psi - ikU''\psi = \frac{k^2 N^2}{\lambda + ikU}\psi \tag{6.32}$$

also called the *Taylor-Goldstein equation*. If we set the Brunt–Väisälä frequency to zero, we recover Rayleigh equation. As for this equation, we shall derive a criterion of stability when the flow is bounded by two horizontal plates. We could, as for Rayleigh's equation, multiply the equation by the conjugate of ψ and integrate z between the two boundaries. We would then get

$$\int_a^b (|d\psi|^2 + k^2|\psi|^2)dz + \int_a^b \frac{ikU''|\psi|^2}{\lambda + ikU}dz = -k^2 \int_a^b \frac{N^2|\psi|^2}{(\lambda + ikU)^2}dz$$

By requiring the cancellation of the imaginary part of this equation, we find the following necessary condition for the instability of the flow:

$$U'' = \frac{2(\lambda_I + kU)kN^2}{\lambda_R^2 + (\lambda_I + kU)^2}$$

where we set $\lambda = \lambda_R + i\lambda_I$. Unfortunately, this equation is not a criterion of the flow itself, unlike Rayleigh's one, since it depends on the eigenvalue. The way to obtain a true criterion on the flow was discovered by L. Howard in 1961. It consists in making use of the function

$$\chi = \frac{\psi}{\sqrt{\lambda + ikU}}$$

which obeys

$$D\left[(\lambda + ikU)D\chi\right] + \left[k^2 \frac{U'^2/4 - N^2}{\lambda + ikU} - \frac{ikU''}{2} - k^2(\lambda + ikU)\right]\chi = 0 \tag{6.33}$$

which we can multiply by χ^* and integrate between a and b. Taking the real part of the result, we thus find

$$\lambda_R \int_a^b \left\{ |D\chi|^2 + k^2|\chi|^2 - k^2 \frac{U'^2/4 - N^2}{|\lambda + ikU|^2} |\chi|^2 \right\} dz = 0$$

In this equation the integral can vanish if, and only if, $U'^2/4 - N^2 > 0$, or if

$$\mathrm{Ri} = \frac{N^2}{U'^2} \le \frac{1}{4} \tag{6.34}$$

Ri is called *the Richardson number*. Equation (6.34) is generally called the *Richardson's criterion.* We see that it is a necessary condition for instability. For certain particular flows it is also sufficient. This criterion shows that when the stratification is sufficiently large, that is to say when the Brunt–Väisälä frequency is sufficiently high, the flow is stable.

This criterion, like Rayleigh's criterion, can be recovered on heuristic arguments, which allow a more physical understanding. To do this, we shall take two fluid elements respectively at z and $z + \delta z$. In order to exchange them, some work against the buoyancy force must be provided, namely

$$W = -g\delta\rho\delta z$$

The energy will be taken from the reservoir of kinetic energy, which stays in the original flow. We then make the following transformation:

$$\begin{array}{ccc} z + \delta z & \rho + \delta\rho & U + \delta U \\ z & \rho & U \end{array} \longrightarrow \begin{array}{cc} \rho & U + \alpha\delta U \\ \rho + \delta\rho & U + (1-\alpha)\delta U \end{array}$$

where α is a free number between 0 and 1. We see that this transformation conserves the mass and momentum at first order. Let us now calculate the difference of kinetic energy δE_c between the initial and final states. We have

$$\begin{aligned} 2\delta E_c &= \rho U^2 + (\rho + \delta\rho)(U + \delta U)^2 - \rho(U + \alpha\delta U)^2 - (\rho + \delta\rho)(U + (1-\alpha)\delta U)^2 \\ &= 2\alpha(1-\alpha)\rho\delta U^2 + 2\alpha U\delta\rho\delta U \end{aligned}$$

We observe that if $\alpha < 1$ then $\alpha(1-\alpha) \le 1/4$, and the maximum is reached at $\alpha = 1/2$, so that

$$2\delta E_c \lesssim \frac{1}{2}\rho(\delta U)^2 + 2U\delta U\delta\rho\,. \tag{6.35}$$

Because of these constraints, stability is insured if

$$\frac{1}{4}\rho\delta U^2 + U\delta U\delta\rho \leq -g\delta\rho\delta z$$

that is to say if the maximum variation of the kinetic energy is smaller than the work needed to exchange two fluid elements. Finally, there is stability if

$$\frac{1}{4}\left(\frac{dU}{dz}\right)^2 \leq -\frac{g}{\rho}\left(\frac{d\rho}{dz}\right) - \frac{U}{\rho}\frac{d\rho}{dz}\frac{dU}{dz}$$

We shall see later that in many circumstances, stratified flows can be computed using the Boussinesq approximation, which implies the neglect of ρ variations while maintaining constant the product $g\delta\rho$, (buoyancy force must not disappear!). Thus, the second term of the right-hand side is usually negligible compared to the first; in this way, we recover Richardson's criterion, which was discovered in 1920 (see Richardson 1920).

6.3.5 *The Bénard-Marangoni Instability* ♠

At the turn of the twentieth century Bénard (1874–1939) discovered that a thin film of liquid heated from below exhibits some vortical cellular motions. For almost 60 years, these fluid flows have been interpreted as the result of thermal convection, an instability driven by the buoyancy force (this is the subject of our next chapter). However, Pearson (1958) showed that when the fluid layer is very shallow, buoyancy effects are dominated by surface tension effects that are able, as we shall see, to destabilize the fluid at rest.[4]

To understand this phenomenon, we consider a fluid layer of thickness d, infinite in the x and y directions. In the z direction, i.e. across the layer, some temperature gradient is imposed, for instance by heating the bottom boundary. In the equilibrium situation, we thus have

$$T_{\rm eq} = T_0 + \beta z,$$

for the temperature field. We assume that the density variations are negligible altogether, thus perturbations of the velocity field $\mathbf{v}$, of the pressure field δp and of the temperature field δT, verify

[4]The name of Carlo Marangoni (Pavia 1840–Firenze 1925) is generally associated with this instability as he was the first physicist to describe fluid flows driven by surface tension gradients (with a paper in Annalen der Physik in 1871).

$$\begin{cases} \nabla \cdot \mathbf{v} = 0 \\[2ex] \dfrac{\partial \mathbf{v}}{\partial t} = -\dfrac{1}{\rho}\nabla \delta p + \nu \Delta \mathbf{v} \\[2ex] \dfrac{\partial \delta T}{\partial t} + \mathbf{v} \cdot \nabla T_{\mathrm{eq}} = \kappa \Delta \delta T \end{cases} \tag{6.36}$$

These equations need to be completed by boundary conditions. On the bottom plane, we impose no-slip boundary conditions for the velocity and a fixed temperature; thus

$$\mathbf{v} = \mathbf{0} \qquad \text{and} \qquad \delta T = 0 \quad \text{on} \quad z = 0$$

On the top boundary the fluid (a liquid) meets another fluid (a gas). Surface tension is therefore important, and above all its temperature dependence. Since the temperature fluctuations are assumed very small, a linear law is valid and sufficient; we take

$$\gamma(T) = \gamma_0(1 + \gamma_T T) \tag{6.37}$$

where γ_0 and γ_T are given by the nature of the liquid-gas interface. Usually, $\gamma_T < 0$ since surface tension decreases with temperature.[5]

We also assume that the deformation of the interface is negligible (γ_0 is large enough), and neglect the effects of gas motion. In these circumstances, the boundary conditions on the liquid at the interface are that the vertical velocity of the liquid vanishes there and that no horizontal stress applies on this surface. From (1.70), it turns out that:

$$\mathbf{v} \cdot \mathbf{e}_z = 0 \qquad \text{and} \qquad ([\sigma_{\mathrm{liq}}]\mathbf{e}_z - \nabla\gamma) \times \mathbf{e}_z = \mathbf{0} \tag{6.39}$$

[5]Surface tension comes from the binding energy of molecules due to their mutual interactions in a liquid. We may expect that at the critical temperature, which is the temperature where the gas and liquid phases are undistinguishable, the surface tension disappears. This remark lead L. Eötvös (1848–1919) to propose that surface tension varies with temperature like

$$\gamma = k(T_c - T)/V^{2/3}$$

Here k is a universal constant for the liquids, V is the volume of one mole and T_c is the critical temperature. This law, which is known as Eötvös rule, is only approximate, but suggests that γ decreases linearly with temperature, as actually observed experimentally. For instance, the following fit

$$\gamma = 7.3\,10^{-2}\,[1 - 0.0023(T - 291)] \;\; \mathrm{N/m} \tag{6.38}$$

matches rather well the variations of surface tension of water in the range 273–373 K, as illustrated in Fig. 6.4.

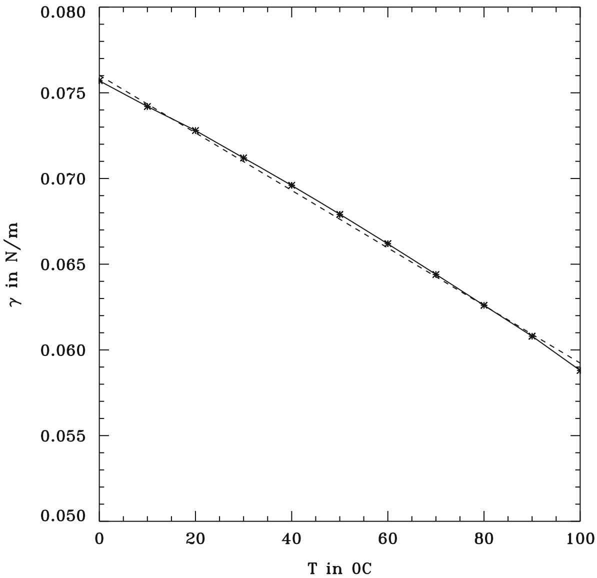

Fig. 6.4 Temperature variations of the surface tension of pure water; the *dashed line* shows the linear fit given in the text

One condition remains to be specified: that on the temperature at the interface. There, we should impose the general conditions between two conducting materials, namely (1.66), with the additional point that air is a transparent medium where energy may be carried out by radiation. Assuming that the liquid radiates like a black body into the gas, boundary conditions at the interface read:

$$T_l = T_g \qquad \text{and} \qquad -\chi_l \frac{\partial T_l}{\partial z} = \sigma T_l^4 - \chi_g \frac{\partial T_g}{\partial z}$$

where σ is Stefan constant. If we now consider the temperature perturbations around a steady state, these perturbations verify:

$$\delta T_l = \delta T_g \qquad \text{and} \qquad \frac{\partial \delta T_l}{\partial z} + q\delta T_l = \frac{\chi_g}{\chi_l}\frac{\partial \delta T_g}{\partial z}$$

Usually, the thermal conductivity of liquids is much higher than the one of gases (see Table 1.1) so that we can safely neglect the right-hand side of the second condition. $q = 4\sigma T_l^3/\chi_l$ is a parameter which measures the efficiency with which the heat flux permeating the liquid is radiated. If the liquid is a good conductor then the gradient of temperature fluctuation must be small near the boundary. Hence, we shall take

$$\frac{\partial \delta T}{\partial z} + q\delta T = 0 \quad \text{on} \quad z = d \tag{6.40}$$

as the boundary condition on the temperature of the liquid at the interface. The remaining condition $\delta T_l = \delta T_g$ is useful only in the case we are interested in the gas temperature fluctuations.

We have now prescribed all the equations and boundary conditions, which control the fate of perturbations. We shall rewrite them using non-dimensional variables. We choose the thickness of the layer as the length scale and d^2/κ as the time scale. The temperature scale is naturally given by $d|\beta|$. Furthermore, as we are making a global analysis of stability, we impose that disturbances evolve as $\exp(\lambda t)$; hence we write the equations of motion:

$$\begin{cases} \nabla \cdot \mathbf{u} = 0 \\ \lambda \mathbf{u} = -\nabla p + \mathcal{P}\Delta \mathbf{v} \\ \lambda T - u_z = \Delta T \end{cases} \tag{6.41}$$

since we take $\beta < 0$. $\mathcal{P}$ is the Prandtl number of the liquid. Using the equation of continuity together with the $\mathbf{u} = \mathbf{0}$ conditions, we derive the following boundary conditions on the $z = 0$ plane:

$$u_z = \frac{\partial u_z}{\partial z} = 0 \qquad \text{and} \qquad T = 0 \quad \text{on} \quad z = 0 \tag{6.42}$$

On the $z = 1$ plane, we should first make the stress condition (6.39) more explicit; it yields

$$\mu\left(\frac{\partial v_z}{\partial x} + \frac{\partial v_x}{\partial z}\right) - \gamma_0\gamma_T\frac{\partial \delta T}{\partial x} = 0, \quad \mu\left(\frac{\partial v_z}{\partial y} + \frac{\partial v_y}{\partial z}\right) - \gamma_0\gamma_T\frac{\partial \delta T}{\partial y} = 0 \quad \text{on } z = 1$$

These conditions are completed by $v_z = 0$. Using dimensionless variables, and mass conservation, the three top boundary conditions give

$$u_z = 0, \qquad \frac{\partial^2 u_z}{\partial z^2} - \mathrm{Ma}\left(\frac{\partial^2 T}{\partial x^2} + \frac{\partial^2 T}{\partial y^2}\right) = 0 \tag{6.43}$$

where we introduced the *Marangoni number*:

$$\mathrm{Ma} = \frac{\gamma_0|\gamma_T||\beta|d^2}{\mu\kappa} \tag{6.44}$$

Finally, the boundary condition on temperature at $z = 1$ reads

$$\frac{\partial T}{\partial z} + \mathrm{Bi}\, T = 0 \tag{6.45}$$

where Bi is the Biot number[6]

$$\mathrm{Bi} = \frac{4\sigma T_{\mathrm{eq}}^3(d)d}{\chi}$$

The system (6.41) can be further reduced to two equations controlling the vertical velocity and the temperature fluctuations; namely:

$$\begin{cases} \lambda \Delta u = \mathcal{P} \Delta \Delta u \\ \lambda T = u + \Delta T \end{cases} \tag{6.46}$$

where $u \equiv u_z$. Since the fluid layer is infinite in the x and y directions, we may express the functions $f(x, y, z) = f(z) \exp(ik_x x + ik_y y)$ and set $k^2 = k_x^2 + k_y^2$. Thus,

$$\begin{cases} \mathcal{P}(D^2 - k^2)^2 u = \lambda(D^2 - k^2)u \\ (D^2 - k^2)T + u = \lambda T \end{cases} \tag{6.47}$$

where $D = \partial/\partial z$. This is a system of sixth order, which is completed by the six boundary conditions:

$$\begin{cases} u = Du = T = 0 & \text{at} \quad z = 0 \\ u = D^2 u + k^2 \mathrm{Ma}\, T = DT + \mathrm{Bi}\, T = 0 & \text{at} \quad z = 1 \end{cases} \tag{6.48}$$

The stability of the fluid layer is determined by the set of eigenvalues λ. It may be shown that the λ's are all real negative numbers when the Marangoni number is zero, hence the system is stable. When this number is increased, the real part of the least-damped mode vanishes for some critical value Ma_c of the Marangoni number. We assume that the associated eigenvalue remains real (the instability is assumed not to be oscillatory). Thus doing, when $\mathrm{Ma} = \mathrm{Ma}_c$, $\lambda = 0$, and we can determine the solutions at the threshold of instability.

The solution of $(D^2 - k^2)^2 u = 0$ verifying $u(0) = Du(0) = u(1) = 0$ is

$$u(z) = A\left[\sinh(kz) + (k \coth k - 1)z \sinh(kz) - kz \cosh(kh)\right]$$

[6] The Biot number is the ratio of two heat transfer coefficients. The heat transfer coefficient is a flux surface density divided by a temperature; for instance, χ_l/d is the heat transfer coefficient of the liquid layer, while σT^3 is that of the vacuum.

We also find that

$$T(z) = \frac{1}{4}\left\{\frac{3}{k}z\cosh(kz) + \frac{k\cosh k - \sinh k}{k\sinh k}\left(z^2\cosh(kz) - z\frac{\sinh(kz)}{k}\right) - z^2\sinh(kz) - \frac{k^2\sinh^2 k + (\mathrm{Bi}+1)A(k)}{k^2\sinh k(k\cosh k + \mathrm{Bi}\sinh k)}\sinh(kz)\right\}$$

where $A(k) = k^2 + k\sinh k\cosh k + \sinh^2 k$. This solution verifies the boundary conditions $T(0) = 0$ and $DT(1) + \mathrm{Bi}T(1) = 0$. Using these two solutions we can express the Marangoni number as a function of the wavenumber k, as:

$$\mathrm{Ma}(k, \mathrm{Bi}) = \frac{8k(k - \sinh k\cosh k)(k\cosh k + \mathrm{Bi}\sinh k)}{k^3\cosh k - \sinh^3 k} \tag{6.49}$$

This function, plotted in Fig. 6.5 for various values of Bi, determines the minimum value of Ma beyond which the instability sets in. We note that, in the ideal case where $\mathrm{Bi} = 0$, the critical value of the Marangoni number is $\mathrm{Ma}_{\mathrm{crit}} = 79.607$ reached at a wavenumber of $k_{\mathrm{crit}} = 1.993$.

As we mentioned it at the beginning of this section, this instability has long been confused with the Rayleigh–Bénard instability, which is driven by the buoyancy

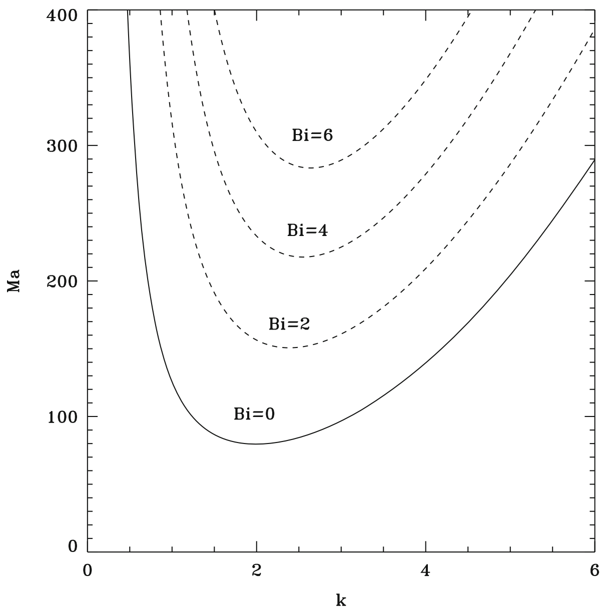

Fig. 6.5 Critical curves for Marangoni-Bénard instability for various values of the Biot number

force. However, as we shall see now, when the thickness of the layer is small enough, the surface tension instability dominates over the buoyancy driven one.

Anticipating on the following chapter, we note that the Rayleigh–Bénard instability is controlled by the Rayleigh number

$$\mathrm{Ra} = \frac{\alpha|\beta|gd^4}{\nu\kappa}$$

which critical value, in similar conditions,[7] is 669.

The dependence of the Rayleigh number with the fourth power of the thickness of the layer, shows that for increasing values of d, the supercriticality of the Rayleigh–Bénard instability is growing faster than that of the tension driven instability, which grows only with the square of the thickness.

We may compute the thickness where the two instabilities are of similar strength. The critical thickness for the tension driven instability is

$$d_t = \left(\frac{\mathrm{Ma}_{\mathrm{crit}}\rho\nu\kappa}{\gamma_0|\gamma_T\beta|}\right)^{1/2}$$

whereas it is

$$d_b = \left(\frac{\mathrm{Ra}_{\mathrm{crit}}\nu\kappa}{\alpha g|\beta|}\right)^{1/4}$$

for the buoyancy driven one. For a given fluid under a similar temperature gradient, these two thicknesses are equal at:

$$d_{\mathrm{bt}} = \sqrt{\frac{\mathrm{Ra}_{\mathrm{crit}}\gamma_0|\gamma_T|}{\mathrm{Ma}_{\mathrm{crit}}\alpha g\rho}}$$

As a numerical illustration, let us consider the case of pure water around 20 °C. At this temperature $\alpha = 2.07 \times 10^{-4}\,\mathrm{K}^{-1}$, and using the linear fit of the surface tension (6.38), we find that the critical thickness is 2.6 cm. Hence, a water layer a few millimeters thick is destabilized by surface tension when heated from below.

6.4 Waves Interaction ♠

Another way to tackle instabilities is to interpret their development as the consequence of the interaction of two waves with energies of opposite sign. The total energy of the system stays constant but the amplitude of the two waves can increase

[7] This means the same boundary conditions on the bottom plate and on the top plate, stress-free and fixed-flux conditions (this is for the case $\mathrm{Bi} = 0$).

indefinitely (in a linear regime, of course!). This approach has been introduced in Fluids Mechanics by Cairns (1979), who adapted technics devised in plasma physics.

6.4.1 The Energy of a Wave

There is no universal definition of the energy of a wave. Following Cairns' work, we shall define it as the work needed to make its amplitude increase from zero to a given finite value A_0. We assume that the passing wave causes a small displacement of matter, which we denote by

$$\xi(x,t) = A(t)e^{i(\omega_0 t - k_0 x)} \ . \tag{6.50}$$

The associated pressure disturbance has a similar form. The function $A(t)$ is assumed to vary slowly: the amplitude of the wave increases very progressively. We express this "slowness" by claiming that

$$\frac{1}{A}\frac{dA}{dt} \ll \omega_0 \qquad \Longrightarrow \qquad \dot{\xi} \simeq i\omega_0 \xi \ .$$

In order to define the work done to raise the wave, we assume that the displacement (6.50) is the result of the action of the pressure forces, which act on both sides of a surface. As long as the wave is not established, the pressure on both sides differs; thus the work reads

$$W = \int_{-\infty}^{+\infty} (p_2 - p_1)\dot{\xi}\, dt$$

or, in complex notations,

$$W = \frac{1}{2} Re \left\{ \int_{-\infty}^{+\infty} (p_2 - p_1)^* \dot{\xi}\, dt \right\} = Re \left\{ \frac{i\omega_0}{2} \int_{-\infty}^{+\infty} (p_2 - p_1)^* \xi\, dt \right\}$$

In a linear problem, all quantities are proportional and therefore we can write

$$\begin{cases} p_1 = D_1(\omega, k_0)A(t)e^{i(\omega_0 t - k_0 x)} \\ p_2 = D_2(\omega, k_0)A(t)e^{i(\omega_0 t - k_0 x)} \end{cases} \tag{6.51}$$

let

$$(p_2 - p_1)^* = D(\omega, k_0)A(t)e^{-i(\omega_0 t - k_0 x)}$$

where $D(\omega, k) = D_2(\omega, k) - D_1(\omega, k)$. When the wave is established, $p_1 = p_2$ and $D(\omega, k) = 0$ is the dispersion relation of the waves system.

Let us calculate the Fourier Transform of $(p_2 - p_1)^*$; we have

$$\Delta \tilde{p}(\omega) = \int D(\omega, k_0) A(t) e^{-i(\omega_0 t - k_0 x)} e^{i\omega t} dt = D(\omega, k_0) e^{ik_0 x} \tilde{A}(\omega - \omega_0)$$

Since A varies slowly with t, $\tilde{A}(\omega - \omega_0)$ differs from zero only at low frequencies, that is to say for $\omega - \omega_0 \approx 0$. In the neighbourhood of ω_0, we have

$$D(\omega, k) = D(\omega_0, k_0) + (\omega - \omega_0) \left(\frac{\partial D}{\partial \omega} \right)_{\omega_0} + \cdots$$

with $D(\omega_0, k_0) = 0$, therefore

$$(p_2 - p_1)^*(t) = e^{ik_0 x} \int \tilde{A}(\omega - \omega_0) D(\omega, k) e^{-i\omega t} d\omega \ ;$$

taking into account our remark about A, this integral is approximated by

$$\begin{aligned}
(p_2 - p_1)^*(t) &= \left(\frac{\partial D}{\partial \omega} \right)_{\omega_0} e^{i(k_0 x - \omega_0 t)} \int (\omega - \omega_0) \tilde{A}(\omega - \omega_0) e^{-i(\omega - \omega_0)t} d\omega \\
&= -i \left(\frac{\partial D}{\partial \omega} \right)_{\omega_0} e^{i(k_0 x - \omega_0 t)} \frac{dA^*}{dt}
\end{aligned}$$

From which we find that

$$W = \frac{\omega_0}{2} \left(\frac{\partial D}{\partial \omega} \right)_{\omega_0} \int_{-\infty}^{+\infty} Re(A \frac{dA^*}{dt}) dt = \frac{\omega_0}{4} \left(\frac{\partial D}{\partial \omega} \right)_{\omega_0} |A_0|^2$$

The energy of a wave is therefore defined by

$$\mathcal{E} = \frac{\omega_0}{4} \left(\frac{\partial D}{\partial \omega} \right)_{\omega_0} |A_0|^2 \tag{6.52}$$

6.4.2 Application to the Kelvin–Helmholtz Instability

We now apply the preceding calculations to the Kelvin–Helmholtz instability studied previously.

The dispersion relation (6.25) shows that two waves corresponding to $\omega_\pm$ are possible. We easily calculate their energy

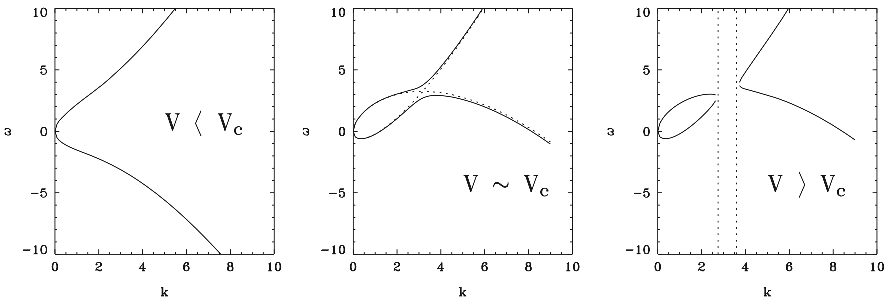

Fig. 6.6 Change of the dispersion relation with the background velocity in a set-up prone to Kelvin–Helmholtz instability. We see that as the background velocity gets close to the critical velocity, a negative energy branch narrows the positive energy one. In the third plot, where $V > V_c$, unstable modes have imaginary frequencies and their wavenumber belongs to the interval limited by the *dotted lines*

$$\mathcal{E}_{\pm} = \omega_{\pm} \left(\frac{\partial D}{\partial \omega} \right)_{\omega_{\pm}} = 2\omega_{\pm}(\omega_{\pm} - \rho_a kV) = \pm 2\omega_{\pm}\sqrt{\Delta}$$

It therefore follows that for every $k > 0$, $\omega_+ > 0$ and $\mathcal{E}_+ > 0$. If $V \ll V_{\rm crit}$ then $\omega_- < 0$ and $\mathcal{E}_- > 0$; the energy of the two waves are of the same sign. However, if $V \lesssim V_{\rm crit}$, there appears a band of wavenumbers k for which $\omega_- > 0$ and thus associated with negative energy waves. Moreover, there exists a wavenumber ($k \sim 3$), such that the two waves are close to resonance, i.e. $\omega_+ \simeq \omega_-$. As illustrated in Fig. 6.6c, this resonance is at the origin of the band of unstable waves.

6.5 The Nonlinear Development of an Instability

Up to now we have studied the evolution of disturbances with infinitesimal amplitudes and noted their exponential growth in the case of instability. Obviously, this growth cannot continue indefinitely because the increasing amplitude inevitably leads to non-negligible nonlinear terms. Their role might simply be to trigger the damping of the instability and to insure a new equilibrium: this is the most simple case that we shall find again in thermal convection in Chap. 7. In general, the situation is more complex: for example, it often happens that a group of modes are unstable because of the set-up. The question we are faced with then is to know towards which solution the system is evolving: is it systematically towards the mode with the highest growth rate? or is it that the nonlinear terms will decide the choice of the final solution which, if it exists, should be stable? It is also possible that no stable solution exists. If the system is chaotic, it wanders indefinitely without ever returning to a point (in the phase space) previously visited.

The nonlinear development of instabilities is a vast field, which would deserve an entire book. The object of this section is thus more modest: we shall examine a few of the simplest cases from which we can shape our intuition about the possible developments of an instability.

6.5.1 Amplitude Equations

When we discussed global instabilities, we expressed the growth of disturbances in the form:

$$\frac{\partial \mathbf{u}}{\partial t} = \mathbf{L}(\mathbf{u})$$

by choosing a time dependence in $e^{\lambda t}$. We generalize this approach by writing

$$\mathbf{u}(\mathbf{r}, t) = A(t)\mathbf{u}_0(\mathbf{r}) \tag{6.53}$$

where $A(t)$ is the amplitude of the mode $\mathbf{u}_0$. If A is very small, we always have

$$\dot{A}(t)\mathbf{u}_0 = A(t)\mathbf{L}(\mathbf{u}_0)$$

but since $\mathbf{u}_0$ is an eigenmode, $\mathbf{L}(\mathbf{u}_0) = \lambda \mathbf{u}_0$, A thus evolves according to

$$\dot{A}(t) = \lambda A(t) \tag{6.54}$$

Such an equation is called an *amplitude equation*. This one is the simplest and its solution $A = A_0 e^{\lambda t}$ is already known to us.

Now, let us suppose that $\mathbf{u}$ is always in the form (6.53), but that its growth is determined by a nonlinear equation that we may write

$$\dot{A}(t) = f(A) \tag{6.55}$$

But for small amplitudes, we have

$$f(A) = f(0) + f'(0)\,A + \frac{f''(0)}{2}A^2 + \frac{f'''(0)}{6}A^3 + \cdots \tag{6.56}$$

Since A is the amplitude of a disturbance, $A = 0$ should be the equilibrium solution such that $f(A = 0) = 0$; therefore, $f(0) = 0$. Further identification shows that $f'(0) = \lambda$. Hence, we rewrite the preceding equation as:

$$\dot{A}(t) = \lambda A + \frac{f''(0)}{2}A^2 + \frac{f'''(0)}{6}A^3 + \cdots \tag{6.57}$$

We can still progress in the determination of the coefficients of the Taylor expansion of f by using the symmetries of the system. Imagine that the system is invariant in the symmetry $A \to -A$, i.e. if A is a solution, $-A$ is also a solution, then it is obvious that $f(-A) = -f(A)$ because of the linearity of ∂_t. In this way all the even derivatives of f are zero and (6.57) shortens to:

$$\dot{A}(t) = \lambda A + \frac{f'''(0)}{6} A^3 + \cdots \tag{6.58}$$

Setting $\mathcal{L} = -f'''(0)/6$, the preceding equation is known as *Landau equation*:

$$\dot{A}(t) = \lambda A - \mathcal{L} A^3 \tag{6.59}$$

and $\mathcal{L}$ is the *Landau constant* of the system(cf. Landau and Lifchitz 1971–1989, Sect. 27).

6.5.2 A Short Introduction to Bifurcations

Landau equation describes the behaviour of many systems in Physics, especially in Fluid Mechanics (we shall meet it again when discussing thermal convection in Chap. 7). Thus, it is worth a little study, which will also allow us to introduce the basic ideas of bifurcation theory. First of all, we shall assume that $\mathcal{L} > 0$.

Assuming $\mathcal{L} > 0$, (6.59) is easily solved: after dividing it by A^3, it is solved for $1/A^2$, which gives

$$A(t) = \frac{A_0}{\sqrt{(1 - A_0^2 \mathcal{L}/\lambda) e^{-2\lambda t} + A_0^2 \mathcal{L}/\lambda}}$$

where A_0 is the amplitude at $t = 0$. Figure 6.7 shows a plot of this solution.

By writing Landau equation in the form

$$\frac{dA}{d\tau} = (\lambda - \mathcal{L} A^2) A\,,$$

we observe that the solution saturates thanks to the term in A^3: the increasing amplitude causes a reduction of the effective growth rate $(\lambda - \mathcal{L} A^2)$. The final amplitude is such that $\lambda - \mathcal{L} A^2 = 0$, or

$$A = A_{eq} = \sqrt{\frac{\lambda}{\mathcal{L}}} \tag{6.60}$$

We see that this solution exists only if $\lambda > 0$. In the opposite case, $A \to 0$. This situation can be summed up by a *bifurcation diagram* (Fig. 6.8) that outlines the

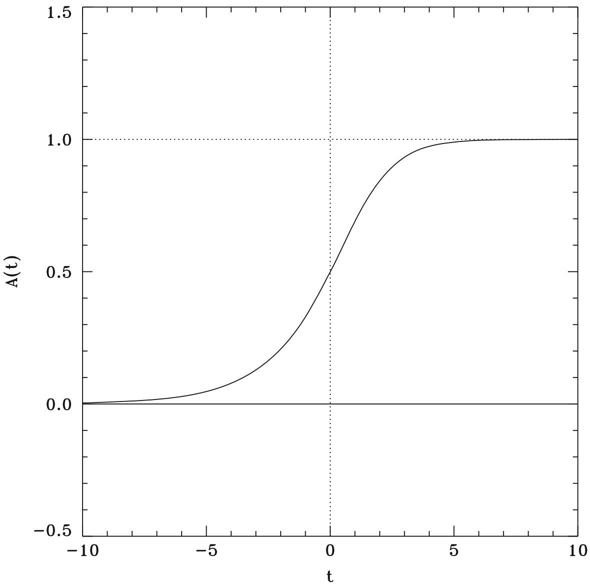

Fig. 6.7 The solution of Landau equation when $\lambda = 0.5$ and $\mathcal{L}/\lambda = 1$

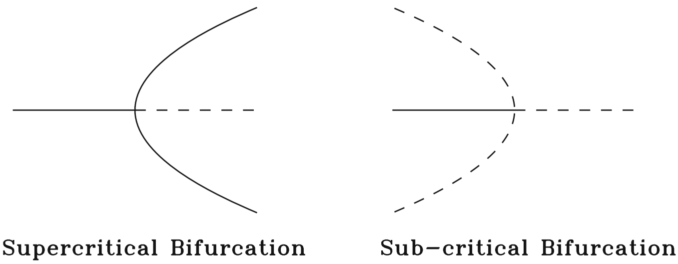

Fig. 6.8 Bifurcation diagrams for Landau equation in the supercritical and sub-critical cases. *Solid lines* indicate stable branches while *dashed lines* are for unstable ones

equilibrium solutions,[8] namely the values of A such that $f(A) = 0$ when the control parameter λ is varied. The control parameter is also known as the *order parameter* in reference to phase transitions, where bifurcations are also playing an important role. In fluid flows, this parameter is usually a number like the Reynolds one.

We now return to Landau equation and its possible equilibrium solutions. $f(A) = 0$ leads to

$$\lambda A - \mathcal{L}A^3 = 0 \quad \Longrightarrow \quad A = 0 \quad \text{or} \quad A = \pm\sqrt{\frac{\lambda}{\mathcal{L}}}$$

[8] The equilibrium solutions are also called fixed points in the language of dynamic systems.

These three solutions constitute the different *branches* of the diagram. It is then necessary to examine their stability. For this, we perturb Landau equation by writing $A = A_{eq} + \delta A$; thus,

$$\frac{d\delta A}{dt} = (\lambda - 3\mathcal{L}A_{eq}^2)\delta A$$

The stability of each branch is given by the sign of $\tau = \lambda - 3\mathcal{L}A_{eq}^2$. If $A_{eq} = 0$, $\tau = \lambda$: the branch is stable if $\lambda < 0$ and unstable if $\lambda > 0$. If $A_{eq} = \sqrt{\lambda/\mathcal{L}}$, the system is in the bifurcated state and its perturbations evolve according to

$$\frac{d\delta A}{dt} = -2\lambda\delta A \tag{6.61}$$

Therefore, when this branch exists (if $\lambda > 0$), it is stable ($-2\lambda < 0$).

The bifurcation controlled by Landau equation is called a *pitchfork bifurcation*. When $\mathcal{L} > 0$, it is *supercritical*. If λ passes from negative values to positive ones, the system bifurcates from a solution that has become unstable ($A_{eq} = 0$) towards a new stable solution ($A_{eq} = \sqrt{\lambda/\mathcal{L}}$). The bifurcation takes place at the critical value $\lambda = 0$.

In some systems, the critical value of λ is not zero but purely imaginary $\lambda = i\omega$: at the bifurcation point the system oscillates with a frequency ω. This kind of bifurcation is called a *Hopf bifurcation*. The behaviour of the system is very similar to the Landau one and we propose its study as an exercise.

Let us now return to Landau equation and consider the case where Landau constant is negative. In this case, non-zero equilibrium solutions exist only if $\lambda < 0$. The bifurcation is called sub-critical and we note from (6.61) that the bifurcated state is always unstable (Fig. 6.8). The evolution from these branches cannot be described by Landau equation (except in an initial phase where the amplitudes are small), because the nonlinear cubic term strengthens the instability rather than reducing it. We should then extend the development of f to the next order in amplitude, namely the one in A^5. This brings us to the consideration of a somewhat more complex system, where we can find a finite amplitude instability.

6.5.3 Finite Amplitudes Instabilities ♠

We shall now analyse a system having a sub-critical bifurcation at $\lambda = 0$ taking into account the A^5-term. The dynamics of the system is assumed to be controlled by the following equation:

$$\frac{dA}{dt} = \lambda A + 2\mathcal{L}A^3 - A^5 \tag{6.62}$$

where the coefficient of A^5 has been set to -1 for simplicity (its negative value is necessary for the instability to saturate). We could also, as we did for Landau equation, explicitly solve this equation but this is not really necessary because the drawing of the bifurcation diagram as well as the analysis of the stability of the different branches allows a good understanding of the dynamics of such a system.

The points of equilibrium are the five solutions that cancel out the right-hand side of (6.62), namely

$$A = 0 \qquad \text{and} \qquad A = \pm\sqrt{\mathcal{L} \pm \sqrt{\mathcal{L}^2 + \lambda}} = \pm A_\pm \tag{6.63}$$

We thus find the axis $A = 0$ plus a fourth-degree curve (see Fig. 6.9). In order to find the stability of the different branches, we must determine the sign of the rate of growth

$$\tau = \lambda + 6\mathcal{L}A^2 - 5A^4$$

for each equilibrium solution. The case of $A = 0$ is immediate. If $A \neq 0$, we can use the equilibrium equation $\lambda + 2\mathcal{L}A^2 - A^4 = 0$ to eliminate λ; recalling the expressions of $A_\pm$ given by (6.63), it turns out that

$$\tau(A_\pm) = \mp 4A^2\sqrt{\mathcal{L}^2 + \lambda}$$

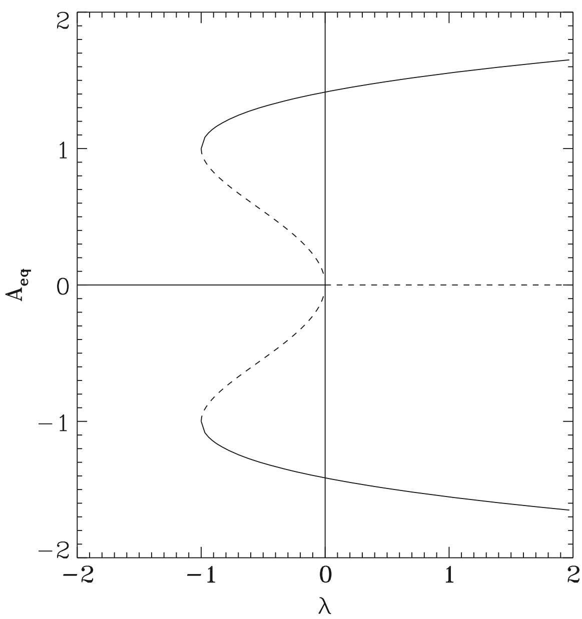

Fig. 6.9 Bifurcation diagram for a system endowed with a subcritical bifurcation obeying (6.62). *Dashed lines* indicate unstable branches, *solid* ones show stables branches (we set $\mathcal{L} = 1$)

then $\tau(A_+) < 0$ and A_+ is stable whereas A_- is unstable since $\tau(A_-) > 0$. The existence of the solutions for $A_\pm$ obviously depends on λ and we may verify that

- A_+ exists if $\lambda \geq -\mathcal{L}^2$,
- A_- exists if $-\mathcal{L}^2 \leq \lambda \leq 0$.

Several conclusions about the dynamics of the system can now be drawn. If $\lambda < -\mathcal{L}^2$, branch $A = 0$ is absolutely stable: whatever the disturbance might be, the system will return to this equilibrium. If $0 > \lambda > -\mathcal{L}^2$ three stable solutions are possible: 0 and $\pm A_+$. The system "will choose" according to initial conditions but henceforth we can note that if the solution $A = 0$ is disturbed strongly enough, we can make it bifurcate towards the other stable branches $\pm A_+$. Although stable with respect to infinitesimal perturbations the solution $A = 0$ is unstable with respect to disturbances of finite amplitude, provided that this amplitude is large enough (the same applies to the branch A_+). We can illustrate this property by noting that the equation of the dynamical system (6.62) can be written using a potential $V_\lambda(A)$ such that

$$\frac{dA}{dt} = -\frac{\partial V_\lambda(A)}{\partial A}$$

The diagram of $V_\lambda(A)$ for different values of λ shows the "valleys" of stabilities and the "peaks" of instability (see Fig. 6.10).

Finally, if $\lambda > 0$, $A = \pm A_+$ are the only stable solutions. Figures 6.9 and 6.10 summarize the properties of this system.

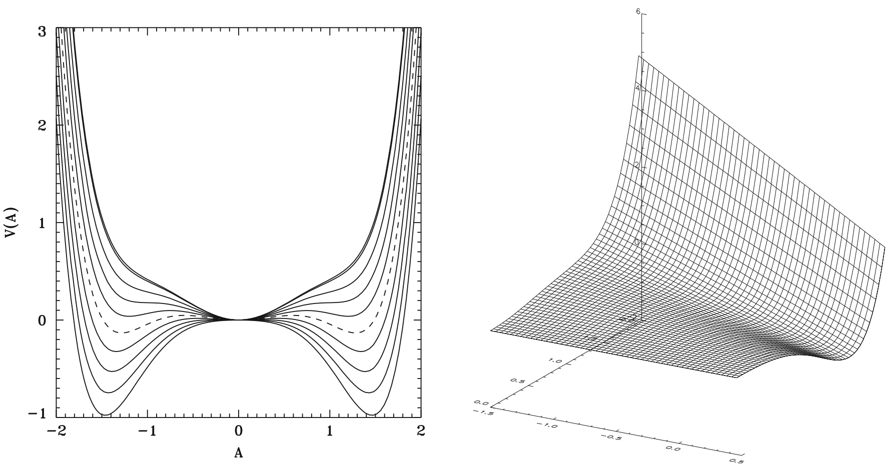

Fig. 6.10 *Left* The potential $V_\lambda(A) = \lambda A^2/2 - \mathcal{L}A^4/2 - A^6/6$ for various values of λ. The *dashed line* shows a value of λ such that $0 > \lambda > -\mathcal{L}^2$ where the potential has three local minima. *Right* A view of the surface $V(A, \lambda)$

6.6 Optimal Perturbations ♠

6.6.1 Introduction

In the foregoing sections we categorized flow disturbances into two families: those of infinitesimal amplitude which are controlled by a linear operator and those of finite amplitude which require the solving of a nonlinear problem. However, on the latter perturbation we discussed only the possible role of a finite amplitude in the context of amplitude equations. We may thus wonder if, like in dynamical systems of Sect. 6.5.3, there exist flows that are stable with respects to infinitesimal perturbations but unstable with respect to some finite amplitudes ones and also wonder how these finite amplitude perturbations are generated. These questions lead us to present a recent progress of Fluid Mechanics that bridges the gap between the two aforementioned categories of disturbances.

Let us first come back to small amplitude perturbations. We decided of the stability of the flow when these perturbations were exponentially damped, that is to say when their temporal evolution was controlled by the $e^{\lambda t}$-factor with $\text{Re}(\lambda) < 0$, the instability criterion being the existence of a perturbation with a positive growth rate. This condition for instability is sufficient of course but not necessary as we shall see. We can indeed imagine the existence of other perturbations that are not described by the eigenvalues of the disturbances operator, like algebraically growing disturbances. One may even imagine situations where a flow is stable as far as perturbations like $f(\mathbf{r})e^{\lambda t}$ are concerned, but that would be transformed into an unstable one by some slowly growing disturbances. This is precisely what has been uncovered in the years 1980: some flows well known to develop turbulence but otherwise known to be stable with respect to small amplitude perturbations have been revealed as the seat of slowly growing perturbations that in the end completely destabilize them. These perturbations are now known as *optimal perturbations*: the linear analysis shows that they can be strongly amplified before disappearing, but during the course of their growth they might transform the original flow into another one that is exponentially unstable.

This scenario shows that finite amplitude disturbances may be spontaneously generated by some small amplitude noise. The existence of optimal perturbations explains why a flow like the cylindrical Poiseuille flow, which is stable linearly for any Reynolds number, shows turbulence bursts when this number is over $\sim 10^3$. In this section we shall introduce the reader to this new page of Fluid Dynamics, a page that has started being written 25 years ago.

6.6.2 Plane-Parallel Flows

Squire theorem told us that two-dimensional perturbations of plane-parallel flows were the most unstable. But three-dimensional ones have other properties, unnoticed for a long time, that might also efficiently control the stability of flows as we shall see.

Let us reconsider the disturbances that might affect a plane-parallel flow $\mathbf{v} = V(z)\mathbf{e}_x$ and let us assume that the fluid is bounded only in the z-direction. We are now considering perturbations of the same shape as (6.13) but we do not impose an exponential time dependance. Thus we write:

$$f(\mathbf{r}, t) = f(z, t)e^{ik_x x + ik_y y} \tag{6.64}$$

for the general form of the perturbations. System (6.18) has now the more general shape:

$$\begin{cases} [\partial_t + ik_x U - \nu(D^2 - k^2)]v_x + v_z U'(z) = -ik_x P \\ [\partial_t + ik_x U - \nu(D^2 - k^2)]v_y = -ik_y P \\ [\partial_t + ik_x U - \nu(D^2 - k^2)]v_z = -DP \\ Dv_z + ik_x v_x + ik_y v_y = 0 \end{cases} \tag{6.65}$$

where $k^2 = k_x^2 + k_y^2$ and $D = \partial_z$. Eliminating pressure and the components v_x and v_y we re-derive Orr–Sommerfeld equation for the vertical velocity v_z:

$$[\partial_t + ik_x U(z) - \nu(D^2 - k^2)](D^2 - k^2)v_z - ik_x U'' v_z = 0 \tag{6.66}$$

We may check that this new form of Orr–Sommerfeld equation gives back (6.23) which we derived previously. Since we now consider three-dimensional perturbations, it is necessary to complete it with an equation for the spanwise v_y component of the velocity. Following tradition, we write the equation verified by the vertical component of the vorticity $\omega_z = \partial_x v_y - \partial_y v_x$. Using the first two equations of (6.65), we easily find that

$$[\partial_t + ik_x U(z) - \nu(D^2 - k^2)]\omega_z + U'(z) ik_y v_z = 0 \tag{6.67}$$

also called *Squire equation*. These two equations form a coupled system whose coupling coefficient is proportional to k_y which represents the variation of perturbations in the third spanwise dimension.

Let us now write Squire and Orr–Sommerfeld equations in the following symbolic form:

$$\frac{\partial}{\partial t}\begin{pmatrix} \Delta v_z \\ \omega_z \end{pmatrix} + \begin{pmatrix} \mathcal{D}_4 & 0 \\ ik_y U' & \mathcal{D}_2 \end{pmatrix}\begin{pmatrix} v_z \\ \omega_z \end{pmatrix} = 0 \tag{6.68}$$

where we introduced the differential operators

$$\Delta = D^2 - k^2, \quad \mathcal{D}_2 = ik_x U(z) - \nu(D^2 - k^2), \quad \mathcal{D}_4 = \mathcal{D}_2(D^2 - k^2)$$

In order to understand the properties of the solutions of this system, it is useful to study a much simpler problem but which shares many of the properties of (6.68).

6.6.3 A Simplified Model

System (6.68) is a differential system where space and time coordinates are coupled. We shall uncouple these variables by forgetting space variations and focusing on time evolution. For that, we consider the following simple system:

$$\frac{d}{dt}\begin{pmatrix} x \\ y \end{pmatrix} = \begin{pmatrix} -\varepsilon & 0 \\ 1 & -2\varepsilon \end{pmatrix}\begin{pmatrix} x \\ y \end{pmatrix} \tag{6.69}$$

where ε is the model parameter. We look for the temporal evolution of $x(t)$ and $y(t)$ whose initial values are (x_0, y_0). The resolution of these two differential equations is straightforward and we find the general solution:

$$\begin{cases} x(t) = x_0 e^{-\varepsilon t} \\ y(t) = (y_0 - x_0/\varepsilon)e^{-2\varepsilon t} + \frac{x_0}{\varepsilon}e^{-\varepsilon t} \end{cases} \tag{6.70}$$

We might observe that at long times ($t \to +\infty$), these solutions vanish for any initial conditions. The short time evolution, that is when $\varepsilon t \ll 1$ is on the contrary sensitive to initial conditions. An expansion of the solution to first order in ε gives

$$x(t) = x_0(1 - \varepsilon t + \mathcal{O}(\varepsilon^2))$$

$$y(t) = x_0(t - \frac{3}{2}\varepsilon t^2 + \mathcal{O}(\varepsilon^2)) + y_0(1 - 2\varepsilon t + \mathcal{O}(\varepsilon^2))$$

These expressions show that $x(t)$ starts decreasing and this is indeed what says the general solution. However, this is not the case for $y(t)$. The first order expansion shows that if $x_0 \gg y_0$, the solution y first increases at a rate controlled by x_0. Obviously, if initial conditions are such that $x_0 \ll y_0$ then $y(t)$ also decreases.

Let us now consider initial conditions where $y(t)$ is increasing with time and search the time t_m where y is maximum. Using the general solution, we easily find that the maximum of y is reached at time

$$t_m = -\frac{1}{\varepsilon}\ln\left(\frac{1 + \varepsilon y_0/x_0}{2}\right)$$

as long as $\varepsilon y_0/x_0 > -1$. If we assume that $x_0 \sim y_0$ and $\varepsilon \ll 1$, we see that

$$t_m \simeq \frac{\ln 2}{\varepsilon}$$

so that the growing of y lasts longer when ε is smaller. y then reaches the amplitude

$$y_m = \frac{x_0}{4\varepsilon}$$

This amplitude is therefore the larger, the longer is the growth. This expression also shows that even if initial perturbations are small, they can be strongly amplified if they are optimally chosen. We shall note however that this condition is not very severe: in the simple case that we are studying we just need to avoid the case $x_0 \ll y_0$. Figures 6.11 and 6.12 illustrate the growth of the y component in the optimal case for various values of ε.

In general the amplification is measured by the energy gain, that is to say by a quadratic function of the amplitude. In our case this gain is simply

$$G(t) = \frac{x(t)^2 + y(t)^2}{x_0^2 + y_0^2} \tag{6.71}$$

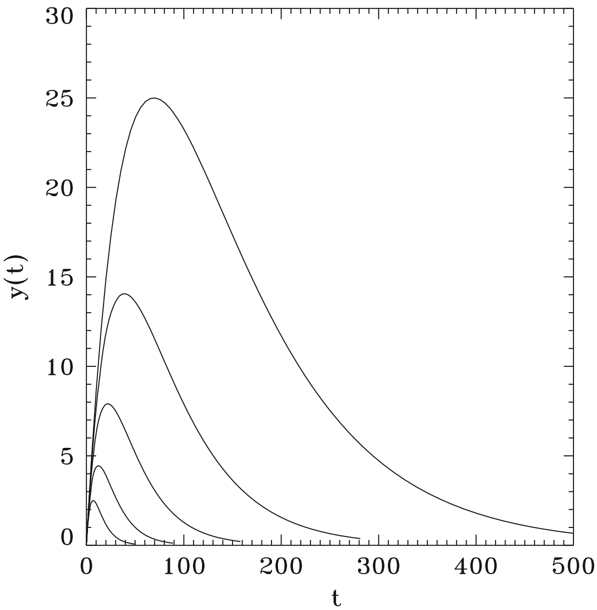

Fig. 6.11 Growth of $y(t)$ for the solution (6.70) for various values of ε with $0.1 \leq \varepsilon \leq 0.01$ when $x_0 = 1$ and $y_0 = 0$. In this case if $t < \ln 2/\varepsilon$ the function is strictly increasing with time. It reaches its maximum $1/4\varepsilon$ at $t = \ln 2/\varepsilon$

For our optimal perturbations verifying $x_0 \gg y_0$, the gain reaches a maximum close to

$$G_{\max} = \frac{1}{16\varepsilon^2}$$

6.6.4 Back to Fluids: Algebraic Instabilities

In view of the foregoing example it is interesting to reconsider system (6.68). We note that if perturbations are such that $k_x \ll 1$, $k_y = \mathcal{O}(1)$ and that ν is small, we qualitatively retrieve the foregoing system. The two diagonal operators are 'small' while the coupling term is of order unity. More rigorously, if $k_x/k_y \sim 1/\mathrm{Re} \ll 1$ we should expect that perturbations are amplified with a gain $\mathcal{O}(\mathrm{Re}^2)$. This is precisely what is found when one solves the full problem of disturbances verifying Orr–Sommerfeld and Squire equations. Table 6.1 illustrates the characteristics of optimal perturbations for a few classical plane-parallel flows. The analogy with the simple system is clear if we set $\varepsilon = 1/\mathrm{Re}$.

The foregoing example shows us the possible existence of perturbations with shear flows whose growth is algebraic. If $\mathrm{Re} \gg 1$, the growth is not limited neither in time neither in amplitude, but like exponentially growing disturbances the nonlinear terms will stop (or modify) this growth. However, algebraic growth is slow compared to an exponential growth. Therefore these perturbations are important when all the eigenmodes are damped. This new type of perturbations redefines the concept of flow stability. Indeed, as soon as these perturbations are able to reach a nonlinear regime they modify the basic flow and represent a true instability of it.

6.6.5 Non-Normal Operators

This non-trivial property of disturbances originates from the nature of the operators that govern their time evolution. Such operators like those of Orr–Sommerfeld–

Table 6.1 The energy gain of a few classical shear flows with the characteristics of the associated optimal disturbances given by the streamwise k_x and spanwise k_y wavenumbers (data are from Schmid and Henningson 2001)

Flow	Gain (10^{-3})	t_{max}	k_x	k_y
Plane Poiseuille	0.20 Re^2	0.076 Re	0	2.04
Plane Couette	1.18 Re^2	0.117 Re	36/Re	1.6
Cylindrical Poiseuille	0.07 Re^2	0.048 Re	0	1
Blasius	1.51 Re^2	0.778 Re	0	0.65

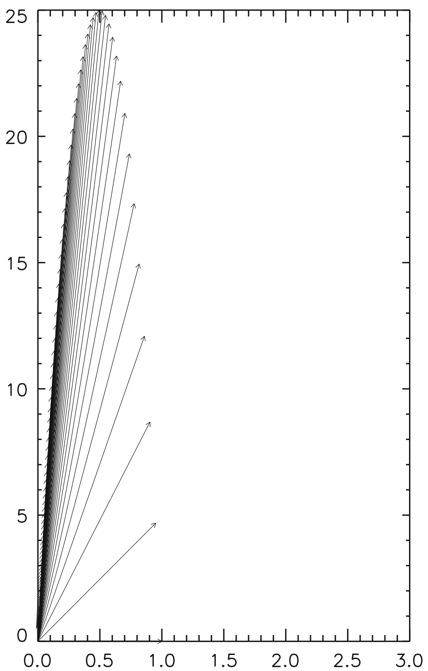

Fig. 6.12 Time evolution of the solution (6.70) when $\varepsilon = 0.01$, $x_0 = 1$ and $y_0 = 0$. Note that the scale in x is strongly dilated compared to that of y

Squire (6.68) are said to be *non-normal*: their eigenfunctions do not make an orthogonal basis (or not even a basis) of summable functions.

Let us consider again our simplified model and compute the eigenvectors associated with the two eigenvalues $-\varepsilon$ and -2ε of the operator. We easily find that these two vectors read:

$$\mathbf{X}_1 = \begin{pmatrix} \varepsilon \\ 1 \end{pmatrix}, \qquad \mathbf{X}_0 = \begin{pmatrix} 0 \\ 1 \end{pmatrix}$$

We note that $\mathbf{X}_1 \cdot \mathbf{X}_2 = 1$. The two eigenvectors are never orthogonal, whatever the value of ε. In addition, when $\varepsilon \to 0$, the two vectors are no longer independent and the matrix can no longer be diagonalized.

In fact it is precisely because the two eigenvectors are never orthogonal that short time growth is possible.

To see this property, we briefly examine the case where the system (6.69) is replaced by

$$\frac{d}{dt}\begin{pmatrix} x \\ y \end{pmatrix} = \begin{pmatrix} -\varepsilon & 0 \\ 0 & -2\varepsilon \end{pmatrix}\begin{pmatrix} x \\ y \end{pmatrix}$$

that is to say when the coupling between components is suppressed. Solutions are then

$$\begin{cases} x(t) = x_0 e^{-\varepsilon t} \\ y(t) = y_0 e^{-2\varepsilon t} \end{cases} \tag{6.72}$$

The energy of these solutions is $E(t) = x_0^2 e^{-2\varepsilon t} + y_0^2 e^{-4\varepsilon t}$ and its temporal derivative is

$$\dot{E}(t) = -2\varepsilon x_0^2 e^{-2\varepsilon t} - 4\varepsilon y_0^2 e^{-4\varepsilon t},$$

which is strictly negative. These solutions are therefore strictly decreasing. Associated eigenvectors are obviously orthogonal.

This remark shows that the coupling term is absolutely essential for the transient growth of $y(t)$ to exist.

6.6.6 Spectra, Pseudo-Spectra and the Resolvent of an Operator

6.6.6.1 Some Definitions

In order to better understand the nature of non-normal operators, it is necessary to get acquainted with some properties of differential operators.

A first important characteristic of a differential operator is its *spectrum.* The spectrum $\sigma(\mathcal{L})$ of the linear operator $\mathcal{L}$ is the set of complex numbers λ such that

$$\lambda \, \mathrm{Id} - \mathcal{L}$$

is not invertible (Id is the identity operator). Its complementary set in $\mathbb{C}$ is called the *resolvent set* $\rho(\mathcal{L})$. It is the set of numbers where the operator

$$R_\lambda = (\lambda \, \mathrm{Id} - \mathcal{L})^{-1},$$

called the *resolvent* of $\mathcal{L}$ is defined.

The spectrum is divided in three parts: the *point spectrum* $\sigma_p(\mathcal{L})$ or *the eigenvalue spectrum*, the *continuous spectrum* $\sigma_c(\mathcal{L})$ and the *residual spectrum.* The residual spectrum $\sigma_r(\mathcal{L})$ is what remains of the spectrum when the point spectrum and the continuous spectrum have been removed.

The point spectrum is the usual set of eigenvalues. It is defined as the set of complex numbers such that

$$\lambda \, \mathrm{Id} - \mathcal{L}$$

is not an injection, namely a function in the image set of the operator may have more than one antecedent by this operator. If we consider the null function, we retrieve the usual property

$$\mathcal{L}(f) = \lambda f$$

of an eigenfunction associated with an eigenvalue λ. The continuous spectrum is the set of complex numbers where $\lambda Id - \mathcal{L}$ is injective but not surjective (the operator is not invertible when λ belongs to the spectrum). The continuous spectrum is not an eigenvalue spectrum and should not be confused with a continuous spectrum of eigenvalues like that of the Rayleigh operator (6.20), which is a set of continuous eigenvalues (i.e. belonging to the point spectrum).

Besides the spectrum, another useful concept is that of the norm of an operator. It is based on the norm of the functions at hands. In Fluid Mechanics, interesting functions are square-integrable functions, namely such that

$$\int_a^b f(x)^2 dx$$

exists. $[a, b]$ is the interval of definition of the function. Such an integral is usually related to the kinetic energy of the system. We thus introduce the norm

$$\|f\| = \sqrt{\int_a^b |f(x)|^2 dx}$$

of a function f. The norm of an operator is defined as

$$\|\mathcal{L}\| = \max_f \left(\frac{\|\mathcal{L}(f)\|}{\|f\|} \right)$$

Mathematics show the following property: for complex numbers z not belonging to the spectrum of $\mathcal{L}$

$$\|(z - \mathcal{L})^{-1}\| \geq \frac{1}{\text{dist}(z, \sigma(\mathcal{L}))} \tag{6.73}$$

Namely, the norm of the resolvent is larger than the inverse of the distance to the spectrum.

We can now introduce the *pseudo-spectrum* $\sigma_\varepsilon(\mathcal{L})$ of the operator $\mathcal{L}$, or rather the ε-pseudospectrum, which is the set of complex numbers z such that

$$\|(z - \mathcal{L})^{-1}\| \geq \varepsilon^{-1} \tag{6.74}$$

6.6.6.2 Physical Interpretation of the Pseudospectrum

Let us consider an operator whose spectrum is only composed of eigenvalues. The norm of its resolvent R_z goes to infinity when z approaches an eigenvalue. z enters the ε-pseudospectrum when the resolvent norm gets over ε^{-1}. The ε-pseudospectrum of an operator $\mathcal{L}$ is therefore a part of the complex plane limited by a contour defined by ε and which surrounds the eigenvalues (see Fig. 6.13).

Normal operators have a pseudospectrum that is in a neighbourhood of the eigenvalues while non-normal operators have a pseudospectrum that extends far away from the eigenvalues.

To give a picture, we may say that non-normal operators have an ill-defined spectrum in the sense that high values of the resolvent occupy large parts of the complex plane. On the contrary a normal operator has a pseudo-spectrum that remains in the neighbourhood of the eigenvalues.

Let us now examine the relation between the non-normality of an operator and the amplification of some disturbances. In order to do so, we consider the following problem:

$$\frac{\partial f(x,t)}{\partial t} = \mathcal{L}(f) \qquad \text{and} \qquad f = f_0(x) \quad \text{at} \quad t = 0$$

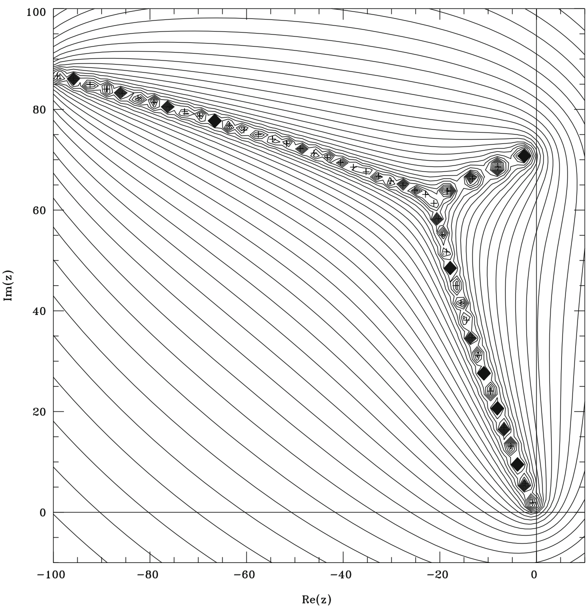

Fig. 6.13 Isocontours of the distance to the eigenvalue spectrum of the Davies operator $\frac{d^2}{dx^2} + (ax^2 - bx^4)$, with $a = 3 + 3i$ and $b = 1/16$. This is a Schrödinger equation with a complex potential. As indicated by (6.73), the ε-pseudospectrum is inside a contour associated with the value $1/\varepsilon$

We shall use the Laplace transform on time, $\tilde{f}$, of function f:

$$\tilde{f}(x,p) = \int_0^\infty f(x,t)e^{-pt}dt$$

Applying Laplace transform to the equation determining f, we get

$$\int_0^\infty \frac{\partial f(x,t)}{\partial t}e^{-pt}dt = \int_0^\infty \mathcal{L}(f)e^{-pt}dt$$

so that

$$\tilde{f} = (p - \mathcal{L})^{-1} f_0 \tag{6.75}$$

The solution for f is then derived from the inverse Mellin–Fourier transform, namely

$$f(x,t) = \frac{1}{2i\pi}\int_{c-i\infty}^{c+i\infty} \tilde{f}(x,p)e^{pt}dp$$

where c is real and larger than the largest real part of the eigenvalues of $\mathcal{L}$.

The foregoing formula shows that the transient response is controlled by the resolvent of $\mathcal{L}$ applied to the initial conditions f_0. If the long time evolution of f is a damping, that is if the eigenvalues of $\mathcal{L}$ are all in the half-plane $Re(z) < 0$, the transient response can nevertheless be large if the operator is non-normal and the initial conditions chosen properly. Indeed, (6.75) shows that the non-normality of the operator is not sufficient. Adapted f_0 are also needed, meaning an optimal choice.

Before ending this section it is interesting to consider another property of the pseudo-spectrum in relation with the stability of flows. Indeed, the pseudospectrum might also be viewed as the union of the spectra of all the operators $\mathcal{L} + \mathcal{E}$ where $\|\mathcal{E}\| \leq \varepsilon$. In other words, if we consider all the possible perturbations of the operator $\mathcal{L}$ by any operator of norm less than ε, the union of all the spectra of these operators defines a part of the complex plane that is identical to the ε-pseudospectrum of $\mathcal{L}$ (Trefethen and Embree 2005). It may well be that $\mathcal{L} + \mathcal{E}$ has unstable modes, namely that perturbing the operator generates exponentially growing modes. This is to say that non-normal operators are sensitive operators: a small change may strongly modify their spectrum.

We here touch finite amplitude perturbations: the small change of the operator (of order ε for its norm) may be viewed as a finite-amplitude disturbance that slightly modifies the background flow. If the operator is normal, nothing happens, but if it is non-normal the new flow may be prone to some exponentially growing modes.

The concept of pseudo-spectrum has many other implications, especially in the numerical calculation of the eigenvalues of matrices where it is associated with the influence of round-off errors (e.g. Valdettaro et al. 2007). We shall stop here the discussion of this subject which would turn into pure mathematics and refer the reader to specialized literature (e.g. Trefethen and Embree 2005).

6.6.7 Examples of Optimal Perturbations in Flows

After this mathematical digression, it is time to reconsider fluid flows. One may wonder if these perturbations actually exist and if they have been observed. As may be guessed from Table 6.1, plane-parallel shear flows are the best candidates for showing such perturbations. The most remarkable example is certainly that of streaks that appear in a boundary layer flow of Blasius type. Figure 6.14 shows the formation of these structures. We note that the flow varies rapidly in the spanwise direction y and slowly in the streamwise direction x. This is just the condition $k_x/k_y \ll 1$.

We may understand the appearance of streaks if we go back to Orr–Sommerfeld and Squire (6.66 and 6.67). If we set $\nu = 0$ and $k_x = 0$ then we get

$$\partial_t u_x = U'(z)u_z \tag{6.76}$$

$$(D^2 - k_y^2)\partial_t u_z = 0 \tag{6.77}$$

the solution of which are of the form

$$\partial_t u_z = Ae^{-k_y z} + Be^{k_y z}$$

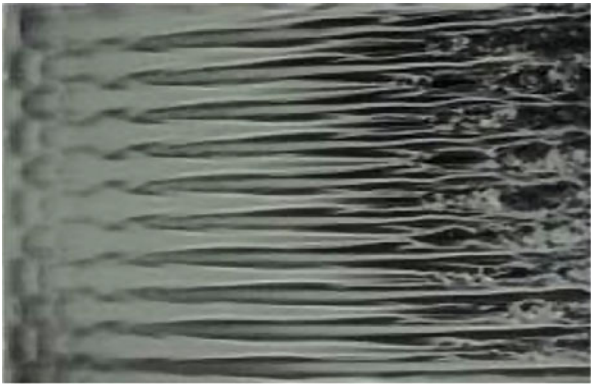

Fig. 6.14 Streaks as a consequence of the lift-up effect in a Blasius boundary layer. The flow is from *left to right*. Note that the disturbance generating the streaks is characterized by a spatial periodicity in the spanwise direction and that the streaks are themselves unstable at some downstream position (Photo by Elofsson and Matsubara, in Elofsson 1998)

but boundary conditions at infinity and at $z = 0$ (namely on the bounding plane) imply that $u_z = 0$ at these two places so that $\partial_t u_z = 0$, or that $u_z = \mathrm{Cst} = u_z(t = 0) = u_z^0$. The first equation (6.76) gives us the time evolution of u_x:

$$u_x = U'(z) u_z^0 e^{ik_y y}\, t \tag{6.78}$$

Hence a disturbance of the vertical velocity, characterized by the wavenumber k_y, generates a local increase of the velocity of the flow in the streamwise direction. This effect is now known as the *lift-up effect*. We indeed observe that u_x may be written

$$u_x = U'(z)\, \Delta z\, e^{ik_y y}$$

where $\Delta z = u_z^0 t$ is the displacement of matter in the z direction induced by the initial perturbation $u_z^0 e^{ik_y y}$. $U'(z)\Delta z$ is just the first variation in z of the background flow:

$$U(z + \Delta z) = U(z) + U'(z)\Delta z$$

The initial perturbation has therefore lifted by Δz the background flow and yielded in $z + \Delta z$ the flow field $U(z) + u_x$ with $u_x = U'(z)u_z^0\, t\, e^{ik_y y}$. This disturbance thus generates streaks of high and small speed whose wavelength is determined by the condition of optimal growth. If the initial conditions are that of a flow disturbed by some white noise, these perturbations emerge in the end.

The lift-up effect has been first described by the work of Ellingsen and Palm (1975). This is the first mechanism that has been recognized as being associated with optimal perturbations. However, there exist other mechanisms like Orr mechanism where a vorticity disturbance controls the dynamics (see Farrell and Ioannou 1993).

6.7 Exercises

1. *The interstellar cloud:* We consider a sphere of radius R filled with an ideal gas of constant density and constant temperature. Establish the condition on the radius which governs the stability of the sphere according to Jeans criterion. Propose a physical interpretation of this criterion. Make a numerical application for an interstellar cloud composed of molecular hydrogen, with a mass of 100 $M_\odot$ and a temperature of 50 K. What is the stability of this cloud if its diameter is 1 or 10 light-years?
2. Let us consider the flow of an inviscid and incompressible fluid such that

$$\mathbf{v} = s\Omega(s)\mathbf{e}_\varphi$$

a) Recall the condition, on $\Omega(s)$, of the stability of this flow with respect to axisymmetric disturbances.
b) We now study the stability of the following flow:

$$\begin{cases} \Omega = 0 & s \le \eta \\ \Omega = A + B/s^2 & \eta \le s \le 1 \\ \Omega = \Omega_0/s^2 & s \ge 1 \end{cases} \tag{6.79}$$

where the constants A and B are such that $\Omega(s)$ is continuous in the whole domain occupied by the fluid.

We are interested in the non-axisymmetric two-dimensional disturbances. The pressure and the velocity perturbations are of the form

$$f(s)e^{im\varphi+\lambda t}$$

while $v_z = 0$.

Give the linearized equations controlling the evolution of disturbances.
c) What boundary conditions are met by the disturbances at the interfaces at $s = \eta$ and $s = 1$?
d) Show that the radial velocity u of the perturbations verify the same differential equation in the three regions and that it can be written

$$\frac{d}{ds}\left(s\frac{d(su)}{ds}\right) = m^2 u \tag{6.80}$$

Note that in each domain, $\frac{\partial(s^2\Omega)}{\partial s} = 2as$ where a is either zero or equal to A.
e) Give the expression of $u(s)$ in each subdomain (one should look for solutions of the type s^α).
f) Determine the form of the pressure perturbations in each domain.
g) Show that the eigenmodes verify the following dispersion relation

$$\left(\lambda + \frac{im\Omega_0}{2}\right)^2 = \Omega_0^2\left[\frac{\eta^{2m}-1}{(1-\eta^2)^2} + \frac{m}{1-\eta^2} - \frac{m^2}{4}\right] \tag{6.81}$$

h) Show that the modes $m = 1$ and $m = 2$ are always stable.

3. *Fjørtoft Theorem.* Extract the real part of (6.21) and show, using (6.22), that equation

$$\int_a^b \left[(|D\psi|^2 + k^2|\psi|^2) + \frac{k^2|\psi|^2 U''(U-A)}{|\lambda + ikU|^2}\right] dz = 0 \tag{6.82}$$

must be verified for any A. Deduce Fjørtoft theorem.

Further Reading

There are two well-known monographs on flow stability. The one of Drazin and Reid (1981), *Hydrodynamic stability* and the one of Chandrasekhar (1961), *Hydrodynamic and hydromagnetic stability*. Drazin and Reid's one is more modern and pedagogical in its presentation. It also discusses the question of nonlinear stability. However, the one of Chandrasekhar is very complete, especially detailed in the derivation and makes a large use of variational principles. For a very recent introduction to instabilities, the reader may also consult *Hydrodynamic Instabilities* by Charru (2011).

On the applications of dynamical systems to Fluid Mechanics, we suggest *Order within chaos* by Bergé et al. (1984), and also *Instabilities, Chaos And Turbulence: An Introduction To Nonlinear Dynamics And Complex Systems*, by Manneville (2004). As far as optimal perturbations are concerned, the reader may deepen the subject with the monograph of Schmid and Henningson (2001) and the recent review of Schmid (2007).

References

Bergé, P., Pomeau, Y. & Vidal, C. (1984). *Order within chaos*. New York: Wiley.

Cairns, R. (1979). The role of negative energy waves in some instabilities of parallel flows. *The Journal of Fluid Mechanics, 92*, 1–14.

Chandrasekhar, S. (1961). *Hydrodynamic and hydromagnetic stability*. Oxford: Clarendon Press.

Charru, F. (2011) *Hydrodynamic Instabilities*. Cambridge: Cambridge University Press.

Drazin, P. & Reid, W. (1981). *Hydrodynamic stability*. Cambridge: Cambridge University Press.

Ellingsen, T. & Palm, E. (1975). Stability of linear flow. *Physics of Fluids, 18*, 487–488.

Elofsson, P. (1998). Experiments on oblique transition in wall-bounded shear flows. Ph.D. thesis, Royal institute of Technology, Stockholm.

Farrell, B. F. & Ioannou, P. J. (1993). Optimal excitation of three-dimensional perturbations in viscous constant shear flow. *Physics of Fluids, 5*, 1390–1400.

Joggerst, C. C., Almgren, A. & Woosley, S. E. (2010). Three-dimensional Simulations of Rayleigh–Taylor Mixing in Core-collapse Supernovae with Castro. *The Astrophysical Journal, 723*, 353–363.

Manneville, P. (2004). *Instabilities, chaos and turbulence: An introduction to nonlinear dynamics and complex systems*. London: Imperial College Press.

Landau, L., Lifchitz, E. (1971–1989). Mécanique des fluides. Mir.

Pearson, J. (1958). On convection cells induced by surface tension. *The Journal of Fluid Mechanics, 4*, 489–500.

Richardson, L. F. (1920). The supply of energy from and to atmospheric eddies. *Royal Society of London Proceedings Series A, 97*, 354–373.

Schmid, P. & Henningson, D. (2001). *Stability and transition in shear flows*. New York: Springer.

Schmid, P. J. (2007). Nonmodal stability theory. *The Annual Review of Fluid Mechanics, 39*, 129–162.

Trefethen, L. & Embree, M. (2005). *Spectra and pseudospectra*. Princeton: Princeton University Press.

Valdettaro, L., Rieutord, M., Braconnier, T. & Fraysse, V. (2007). Convergence and round-off errors in a two-dimensional eigenvalue problem using spectral methods and arnoldi-chebyshev algorithm. *Journal of Applied Mathematics and Computing, 205*, 382–393.